Development/Plasticity/Repair

Atypical Protein Kinase C and Par3 Are Required for Proteoglycan-Induced Axon Growth Inhibition

Seong-il Lee,[1,2] Weibing Zhang,[1] Mayuri Ravi,[1] Markus Weschenfelder,[3] Martin Bastmeyer,[3] and Joel M. Levine[1]

[1]Department of Neurobiology and Behavior and [2]Program in Neuroscience, Stony Brook University, Stony Brook, New York 11794, and [3]Zoology Institute, Department of Cell and Neurobiology, Karlsruhe Institute of Technology, 76131 Karlsruhe, Germany

When the CNS is injured, damaged axons do not regenerate. This failure is due in part to the growth-inhibitory environment that forms at the injury site. Myelin-associated molecules, repulsive axon guidance molecules, and extracellular matrix molecules including chondroitin sulfate proteoglycans (CSPGs) found within the glial scar inhibit axon regeneration but the intracellular signaling mechanisms triggered by these diverse molecules remain largely unknown. Here we provide biochemical and functional evidence that atypical protein kinase C (PKCζ) and polarity (Par) complex proteins mediate axon growth inhibition. Treatment of postnatal rat neurons *in vitro* with the NG2 CSPG, a major component of the glial scar, activates PKCζ, and this activation is both necessary and sufficient to inhibit axonal growth. NG2 treatment also activates Cdc42, increases the association of Par6 with PKCζ, and leads to a Par3-dependent activation of Rac1. Transfection of neurons with kinase-dead forms of PKCζ, dominant-negative forms of Cdc42, or mutant forms of Par6 that do not bind to Cdc42 prevent NG2-induced growth inhibition. Similarly, transfection with either a phosphomutant Par3 (S824A) or dominant-negative Rac1 prevent inhibition, whereas expression of constitutively active Rac1 inhibits axon growth on control surfaces. These results suggest a model in which NG2 binding to neurons activates PKCζ and modifies Par complex function. They also identify the Par complex as a novel therapeutic target for promoting axon regeneration after CNS injury.

Introduction

The growth and guidance of axonal processes during nervous system development is regulated by extracellular cues that attract or repel axonal growth cones (Tessier-Lavigne and Goodman, 1996). After binding to their receptors, these cues activate intracellular second messenger systems that alter the functions of the actin and microtubule-based cytoskeletal motors that control growth cone motility and drive axon extension (Bashaw and Klein, 2010). Many repulsive axon guidance molecules are reexpressed at high levels at CNS injury sites (Yiu and He, 2006). Together with myelin-associated inhibitory molecules and chondroitin sulfate proteoglycans (CSPGs), they create a biochemical barrier to successful axon regeneration. Understanding the mechanisms by which these diverse molecules cause axon growth inhibition may lead to new treatments to promote regeneration after injury.

Severed adult axons must reform a growth cone to regenerate. Peripheral neurons do this successfully, but CNS neurons form dystrophic end bulbs that remain embedded in the glial scar at the injury site (Ramón y Cajal, 1928). Growth cone formation requires the reestablishment of the actin and microtubule based cytoskeletal motors (Bradke et al., 2012). During development, growth cone formation and axonogenesis is regulated by the polarity (Par) complex (Arimura and Kaibuchi, 2007). This complex of atypical PKCζ, Par6, and Par3 is activated by Cdc42, and in turn regulates the location and activity of Rac1. Axonogenesis requires the transport and accumulation of Par3 and Par6 at the tip of the neurite that will become the axon (Shi et al., 2003; Schwamborn and Puschel, 2004; Nishimura et al., 2005) and also requires the activity of PKCζ (Chen et al., 2006). By regulating the organization and coordinating the functions of actin microfilaments and microtubules, the Par complex is necessary for axon specification, growth cone formation, and axon extension.

Here we asked whether the inhibition of axon growth induced by injury-associated molecules involves an alteration of PKCζ and Par complex function. We focused on the NG2 CSPG because it is a major proteoglycan constituent of glial scars (Jones et al., 2002; Tang et al., 2003). NG2 is secreted or shed predominantly from reactive oligodendrocyte precursor cells and reaches maximum levels at injury sites within 5–7 d after injury. NG2 inhibits axon growth *in vitro*, forms barriers to axon extension, and induces growth cone collapse (Dou and Levine, 1994; Fidler et al., 1999; Chen et al., 2002; Ughrin et al., 2003), although these findings remain controversial (Yang et al., 2006a; Busch et al., 2010). After spinal cord injury, the dystrophic ends of damaged axons are embedded in NG2-rich regions of the glial scar (Jones et al., 2002), and the infusion of function-blocking antibodies against NG2 allows sensory axons to grow into and out of an injury site (Tan et al., 2006). Thus, treating neurons *in vitro* with NG2 provides a model system for determining the intracellular

Received July 3, 2012; revised Nov. 26, 2012; accepted Dec. 9, 2012.

Author contributions: S.-i.L., M.B., and J.M.L. designed research; S.-i.L., W.Z., M.R., and M.W. performed research; S.-i.L. analyzed data; S.-i.L., M.B., and J.M.L. wrote the paper.

This work was supported by New York State Spinal Cord Injury Research Board Contract C023081. We thank Drs. H. Geller, S. Ge, and M. Shelly for their comments on this manuscript.

The authors declare no competing financial interests.

Correspondence should be addressed to Joel M. Levine, Department of Neurobiology and Behavior, Stony Brook University, Stony Brook, NY 11794. E-mail: joel.levine@stonybrook.edu.

DOI:10.1523/JNEUROSCI.3154-12.2013

 0270-6474/13/332541-14$15.00/0

mechanisms of axon growth inhibition. Here, we show that the inhibition of axon growth induced by NG2 requires the activation of Cdc42 and PKCζ. This activation results in an alteration in Par complex function. These studies define a novel function for Par3 in axon repulsion and identify a new therapeutic target for encouraging axon regeneration after CNS injury.

Materials and Methods

Antibodies

Anti-PKCζ antibody (sc-216), anti-Rac1 antibody (sc-217), and anti-Myc antibody (sc-40) were purchased from Santa Cruz Biotechnology. Anti-Phospho-PKCζ/λ (9378) antibody was purchased from Cell Signaling Technology. Anti-Par3 antibody (07–330) and anti-Tau (MAB361) was purchased from Millipore. Monoclonal anti-FLAGM2 antibody (F3165) and anti-β-actin antibody (A5316) were purchased from Sigma. Living Colors DsRed polyclonal antibody (632496) was purchased from Clontech. Neuronal Class III β-tubulin (Tuj1) monoclonal antibody was purchased from Covance.

siRNAs

To target endogenous PKCζ, ON-TARGETplus SMARTpool PRCKZ, a mixture of the following different sequences of siRNA targeting rat PKCζ (NM 022507), was purchased from Dharmacon: 5′-CCACGACGAUGAGGAUAUC-3′ (864–882), 5′-UCGGAAACAUGACAAUAUC-3′ (654–672), 5′-UCACACGUCUUGAAAGGAU-3′ (1456–1474), and 5′-CGAUGCCGAUGGACACAUU-3′ (1152–1170).

Scrambled control siRNA was kindly provided by H. Colognato (Stony Brook University, Stony Brook, NY).

Plasmids

pCAG-EGFP. This CMV early enhancer/chicken β actin promoter (CAG)-based plasmid was constructed to overexpress exogenous proteins in primary cells. pCIG2 (a gift from Y. Zou, University of California at San Diego, San Diego, CA) was linearized with MscI, and the resulting 5′ overhang sequences were Klenow-filled. The cassette containing multiple cloning site (MCS), IRES, and EGFP sequences was removed by XhoI digestion. A fragment containing the MCS and EGFP ORF was obtained from pEGFP-N1 (Clontech) by XhoI and NotI digestion and ligated into the linearized pCIG2.

pCAG-PKCζ-EGFP. The ORF of rat PKCζ was amplified by PCR from pHACE-PKCζ (a kind gift from J. So, Inha University, Incheon, South Korea) with the primers 5′-CCGCTCGAGCT GCCACCATGCCCAGC AGGACCGACCCC-3′ and 5′-CGGAATTCTGCACGGA CTCCTCAGC AGACAG-3′ and cloned into the XhoI and EcoRI sites of pCAG-EGFP.

pCAGJC. For pCAGJC, the expression cassette of EGFP in pCAG-EGFP was excised by AgeI and BsrGI digestion. The resulting overhang sequences were filled in with Klenow and self-ligated. This vector was used to clone small epitope-tagged expression cassettes.

pCAGJC-FLAG-PKCζ. The FLAG-tagged mouse PKCζ expression cassette was excised with EcoRI from pCIG2-PKCζ WT (a kind gift from Y. Zou) and subcloned into the same sites of pCAGJC.

pCAGJC-FLAG-PKCζ T410E. To mutate the phosphorylation site of PKCζ, an *in vitro* site-directed mutagenesis kit (Quick Change) from Agilent Technologies was used. pCAGJC-FLAG-PKCζ was PCR-amplified with the primers 5′-GGCCCCGGTGATACAACAAGCGAG TTTTGTGGAACCCCGAACTAT-3′ and 5′-ATAGTTCGGGGTTCCA CAAAACTCGCTTGTTGTATCACCGGGGCC-3. The mutation was confirmed by sequencing analysis.

pCAGJC-FLAG-PKCζ T410/560E. pCAGJC-FLAG-PKCζ T410E was PCR-amplified with the primers 5′-GCGAGCCTGTGCAGCTGGAACC AGATGATGAGGACGTC-3′ and 5′-GACGTCCTCATCATCTGGTTC CAGCTGCACAGGCTCGC-3′. The mutation was confirmed by sequencing analysis.

pCIG2-FLAG-PKCζ K281W (kinase deficiency). pCIG2-FLAG-PKCζ K281W was a kind gift from Y. Zou (Wolf et al., 2008).

pCAGJC-myc-Par6C. For pCAGJC-myc-Par6C, the Myc-tagged human Par6C expression cassette was PCR-amplified from pk-myc-Par6C (Joberty et al., 2000) (Addgene plasmid 15474) with the primers 5′-GC GAGCTCCTGCCACCATGGCCCGGCCGCAGAGGACT-3′ and 5′-CG GAATTCTCAGAGGCTGAAGCCACTACCATC-3′ and cloned into the SacI and EcoRI sites of pCAGJC.

pCAGJC-mycPar6ΔCRIB. The semi-CRIB domain sequence of Myc-tagged Par6C was deleted by using PCR as follows. First, the 5′ fragment of semi-CRIB domain was PCR-amplified with the primers 5′-GCGAGC TCCTGCCACCATGGCCCGGCCGCAGAGGACT-3′ and 5′-CCGTCG GTGGGTCTCAGGCAGTGCCACTGGCCGCAGCAAGAG-3′, and the 3′ fragment with primers 5′-CTCTTGCTGCGGCCAGTGGCACTGCC TGAGACCCACCGACGG-3′ and 5′-CGGAATTCTCAGAGGCTGAA GCCACTACCATC-3′. These two fragments were then adjoined by PCR with the primers GCGAGCTCCTGCCACCATGGCCCGGCCGCAGA GGACT-3′ and 5′-CGGAATTCTCAGAGGCTGAAGCCACTACCA TC-3′ and cloned into the SacI and EcoRI sites of pCAGJC.

pCAGJC-mycPar6Δ135P. For pCAGJC-mycPar6Δ135P, the proline residue at position 135 of Myc-tagged Par6C expression cassette was deleted using PCR. First, the 5′ fragment of semi-CRIB domain was PCR-amplified with the primers 5′-GCGAGCTCCTGCCACCATGGCCCGGCCGCAGA GGACT-3′ and 5′-GGAAACCTGGCGGAAATCTTGCAGGCTGATTAG CAAGGGTGG-3′, and 3′ fragment with primers 5′-CCACCCTTGCTAAT CAGCCTGCAAGATTTCCGCCAGGTTTCC-3′ and 5′-CGGAATTCTC AGAGGCTGAAGCCACTACCATC-3′. These two fragments are adjoined by PCR with the primers 5′-GCGAGCTCCTGCCACCATGGCCCGGCCG CAGAGGACT-3′ and 5′-CGGAATTCTCAGAGGCTGAAGCCACTAC CATC-3′ and cloned into the SacI and EcoRI sites of pCAGJC.

pCAGJC-myc-Par3b. For pCAGJC-myc-Par3b, the expression cassette of Myc-tagged Par3b was cut from pk-myc-Par3b (Joberty et al., 2000) (Addgene plasmid 19388) with HindIII and EcoRI and cloned into the same sites of pCAGJC.

pCAGJC-myc-Par3b S824A. To mutate the PKCζ phosphorylation site of Par3b, pCAGJC-myc-Par3b was PCR-amplified with the primers 5′-GAAG GATTTGGACGTCAGGCTATGTCAGAAAAACGCACA-3′ and 5′-TGTG CGTTTTTCTGACATAGCCTGACGTCCAAATCCTTC-3′. The PCR mixture was treated with DpnI to remove the template strands and used for transformation. The mutation of each plasmid was confirmed by sequencing analysis.

pCAGJC-dTomato. pC1-dTomato (a kind gift form N. Kumamoto, Osaka University, Osaka, Japan) containing a dTomato version of pC1-EGFP (Clontech) was digested by NheI, and the resulting sticky ends were blunted by Klenow. The fragment including the dTomato expression cassette and MCS sequence excised with XmaI and was cloned into the XhoI (Klenow-filled) and XmaI sites of pCAGJC.

pCAGJC-dTom-Cdc42 WT and pCAGJC-dTom-Cdc42 DN(T17N). For pCAGJC-dTom-Cdc42 WT and pCAGJC-dTom-Cdc42 DN(T17N), the Cdc42 expression cassettes of wild-type (WT) and dominant-negative (DN) pcDNA3-EGFP-Cdc42, respectively, were excised by BsrGI and XhoI and then cloned into the same sites of pCAGJC-dTomato.

pCAGJC-dTom-Cdc42CA(Q61L). To mutate the wild type of Cdc42 into the constitutively active (CA) form, pCAGJC-dTom-Cdc42 WT was PCR-amplified with the primers 5′-TTTTTGATACTGCAGGGCTAGA GGATTATGACAGATT-3′ and 5′-AATCTGTCATAATCCTCTAGCC CTGCAGTATCAAAAA-3′. The mutation of each plasmid was confirmed by sequencing analysis.

pCAGJC-dTom-Rac1 WT, pCAGJC-dTom-Rac1DN(T17N), and pCAGJC-dTom-Rac1 CA(G12V). Expression cassettes of wild-type, dominant-negative, and constitutively active Rac1 were amplified from pCMV-HA-Rac1 (a gift from S. Halegoua, Stony Brook University, Stony Brook, NY) by PCR with the primers 5′-CCGCTCGAGCTATGCAGGCCATCA AGTGTGTGG-3′ and 5′-CGGAATTCTTACAACAGCAGGCATTTTC TC-3′ and cloned into the XhoI and EcoRI sites of pCAGJC-dTomato.

Purification of NG2. A recombinant fragment corresponding to the entire extracellular domain (ECD) of NG2 was purified as described previously (Tillet et al., 1997; Ughrin et al., 2003).

Primary culture

Cultures of dissociated cerebellar granule neurons (CGNs) were prepared from newborn rat pups of either sex as described previously (Dou and Levine, 1994). Neurons were plated onto either a glass coverslip coated with 50 μg/ml poly-L-lysine (PLL) and protein substrates or a culture dish coated with 25 μg/ml PLL. Embryonic day 18 Sprague Daw-

ley hippocampi were purchased from BrainBits and dissociated following the manufacturer's protocol. Neurons were plated onto glass coverslips coated with poly-L-lysine or poly-L-lysine plus NG2 CSPG at a density of $5–10 \times 10^3$ cells/cm^2 and cultured at 37°C and 5% CO_2 for 24–48 h.

Adult mouse dorsal root ganglia culture and neurite measurement

Dorsal root ganglia (DRGs) were dissected from 6-week-old mice and treated with dispase II (Roche) and collagenase (Sigma) and titurated. Approximately 1000 cells were plated onto a 15 mm glass coverslip coated with either 50 μg/ml PLL and 2 μg/ml laminin alone (control substrate) or PLL and 2 μg/ml laminin along with 10 μg/ml NG2 ECD (NG2 substrate). Cells were cultured in Neurobasal-A supplemented with B27 (Invitrogen) for 48 h, fixed with 4% paraformaldehyde in 100 mM phosphate buffer, and stained with anti-Tuj1 antibody (1:1000). Cells were visualized using Alexa Fluor 488- or Alexa Fluor 594-conjugated donkey anti-rabbit secondary antibodies (1:1000). To quantify the average neurite length per cell, 5 to 10 fields per coverslip were randomly selected and imaged with fluorescence microscopy (Axio Imager system, Carl Zeiss) for each group. The images of DRGs were binarized and skeletonized with MetaMorph software. The total white pixel numbers of each cell were counted and logged onto an Excel spreadsheet, and the mean number of pixels per cell was calculated.

Immunocytochemistry

Cultures were fixed and stained as described previously (Dewald et al., 2011). Primary antibodies were polyclonal anti-PKCζ (1:200; Santa Cruz Biotechnology), anti-Par3 (1:100; Millipore), monoclonal anti-Tau (1:100; Millipore), Neuronal Class III β-tubulin (Tuj1) monoclonal antibody (1:500; Covance), and anti-GAP43 (1:5000; gift from D. Schreyer, University of Saskatoon, Saskatoon, SK, Canada). Alexa Flour 488- or 594-conjugated donkey anti-mouse or donkey anti-rabbit secondary antibodies (diluted 1:1000, 30 min incubation; Invitrogen) were used to detect the primary antibodies.

For the quantitation of PKCζ and Par3 immunoreactivity, between 1 and 15 *Z*-stack images per cell were acquired with an Olympus FluoView 1000 confocal laser-scanning microscope. FluoView 1000 viewer and MetaMorph software were used for the analysis of each image. For PKCζ, a plane containing a middle part of the cell body was selected and exported for analysis to the MetaMorph software. Pixel intensity distribution was measured across the selected cell body image with the linescan function of MetaMorph software. For Par3, in each acquired cell image, a plane containing the brightest Par3 signal in the axonal compartment was selected, a line was traced along the axon, and its average pixel intensity was measured with the linescan function of MetaMorph. To measure the Par3 signal in the cell body, a circle was traced along the edge of each cell, and the average pixel intensity of the area was measured with the area measurement tool of MetaMorph software. To calculate the Par3 signal ratio between the soma and axon of each cell, the mean pixel intensity of Par3 of the cell body was divided by that the of axon.

Microscopy

Cells were fixed with 4% paraformaldehyde. After washing and staining, cells were mounted in fluorescence mounting medium (Southern Biotech) and stored at 4°C. Cells were imaged by epifluorescence on a Axioplan 2 imaging microscope (Carl Zeiss) with a 20× numerical aperture (NA) 0.75 plan-Apochromat objective. Digital (16 bit) images were acquired with a cooled charge-coupled device (Axiocam; Carl Zeiss) using AxioVision 4.7.2 software.

For confocal laser scanning microscopy, cells were imaged on an FV 1000 confocal microscope (Olympus) equipped with either a 40× (UPlan FL N, 1.30 NA) or 60× (PLAN APO, 1.42 NA) oil-immersion objective. Digital (12 bit) images were acquired with a cooled charge-coupled device using FV10-ASW 2.1 software and processed using MetaMorph software (Molecular Devices).

Neurite outgrowth assay

Neurite outgrowth assay were performed as described previously (Dou and Levine, 1994). Briefly, CGNs were plated at the density of 1×10^4 cells onto a 15 mm glass coverslip treated either with 50 μg/ml PLL and 2 μg/ml laminin alone (control substrate) or PLL and 2 μg/ml laminin along with one of the following: NG2 ECD (10 μg/ml) (Ughrin et al., 2003), neurocan (10 μg/ml) (Asher at al., 2000), aggrecan (10 μg/ml; Sigma), chick brain CSPGs (5 μg/ml; Millipore), or myelin membranes [20–40 μg/ml total protein; prepared according to the procedure of Norton and Poduslo (1973)]. After electroporation, cells were plated, cultured in DMEM containing 10% FBS for 20–24 h, and fixed with 4% paraformaldehyde in 100 mM phosphate buffer. In some cases, the cells were stained with a neuron-specific marker such as β-tubulin III, Tuj1, or anti-GAP43 antibody. In other cases, cells were imaged using the dTomato fluorescence. To quantify neurite lengths, 5 to 10 fields per coverslip were randomly selected and imaged. A neurite was defined as a process extending from the neuronal cell body by more than a cell diameter. Length was measured from the axon initial segment to the tip of neurite using the line measurement tool in MetaMorph (Molecular Devices). For cells that had more than one neurite, only the longest one was measured. In the genetic modification experiments, only transfected cells marked by dTomato expression were counted for analysis. Each experiment was repeated at least three times unless noted otherwise, and comprised duplicate coverslips for each condition. A minimum of 300 cells were measured for each experimental condition.

Transient transfections

The Amaxa Nucleofection system (Lonza) was used to deliver exogenous genes or siRNA into primary neurons. For each nucleofection, 5×10^6 of dissociated CGNs and either 0.75–2.5 μg of plasmid DNA or 10–200 pmole of siRNA was suspended in 100 μl of nucleofection solution and nucleofected with program G-013. The cell suspensions were immediately diluted with 1 ml of DMEM containing 10% FBS, and 50–100 μl of cell suspension was plated onto coated coverslips. For biochemical analysis $2–3 \times 10^7$ cells were plated onto PLL-coated 60 mm culture dishes. HT22 cells, an immortalized mouse hippocampal cell line (Behl et al., 1995), were transfected with 4 μg of plasmid DNA using Lipofectamine 2000 (Invitrogen) according to the manufacturer's instructions.

NG2 treatment, immunoblot, and immunoprecipitation

For biochemical analysis, either 5×10^6 nontransfected CGNs or 1×10^7 transfected CGNs were plated onto each 35 mm culture dish coated with 25 μg/ml PLL and cultured in Neurobasal-A with B27 supplement overnight. HT22 cells were plated 3×10^5 onto 35 mm culture dishes and cultured in DMEM containing 10% FBS overnight. Primary cells were starved in Neurobasal-A without B27 for 3–5 h in the presence or absence of relevant compounds. HT22 cells were starved either in serum-free DMEM for 3–5 h or in Neurobasal-A with B27 overnight followed by Neurobasal-A without B27 for 3–5 h before treatment.

After treatment, the cells were washed twice with cold PBS and lysed in either 0.3% or 1.0% CHAPS lysis buffer (20 mM phosphate buffer, pH 7.4, 150 mM NaCl, 1 mM EDTA, and either 0.3% or 1.0% CHAPS) supplemented with proteinase and phosphatase inhibitor cocktail (Roche). Insoluble fractions were removed by centrifugation at $16,000 \times g$ for 10 min, and soluble fractions were subjected to immunoblotting or immunoprecipitation.

For immunoprecipitation, 1–2 μg of primary antibody and 20 μl of protein G beads (Roche) were added to 100–500 μg of cell lysate and incubated under constant agitation for 2–4 h or overnight at 4°C. The resulting bead-bound immune complexes were washed four times with the lysis buffer, resuspended, and boiled in 25–50 μl of 2× protein sample buffer. The primary antibodies and their dilution ratio were as follows: anti-PKCζ antibody (1:1000), anti-Rac1 antibody (1:1000), anti-Myc antibody (1:1000), anti-phospho-PKCζ/λ antibody (1:1000), anti-Par3 antibody (1:2000), monoclonal anti-FLAG/M2 antibody (1:2000), anti-β-actin antibody (1:50000), and Living Colors DsRed polyclonal antibody (1:2000). The blots were washed and incubated in horseradish peroxidase-conjugated secondary antibodies (1:2000; GE Healthcare) for 30 min to 2 h. Then, the blots were washed, developed with the GE Healthcare ECL kit, and exposed to HyblotCL autoradiograph film (Denville Scientific) to detect specific chemoluminescence.

For the preparation of cytoplasmic and membrane fractions of cells, CGNs were grown overnight on coated tissue cultures dishes, and the monolayers were lysed in 0.02 M Tris-Cl, pH 7.4, 0.25 M sucrose, 10 mM

EGTA, 2 mM EDTA, 10 μg/ml aprotinin and leupeptin, and 0.2 mM PMSF and centrifuged at 130,000 × *g* for 30 min. The resulting pellet was resuspended in the same solution containing 1% Triton X-100, kept on ice for 60 min, and centrifuged again. Protein was determined with the Bradford reagent (Bio-Rad). In some experiments, 2 μM ZIP peptide (cell-permeable pseudosubstrate peptide inhibitor, N-Myr-SIYRRGARRWRKL-OH, Enzo Life Sciences) was added 3 h before lysis, or cells were treated with phorbal-12-myrisate-13-acetate (PMA; 200 nM) for 5 min before lysis.

Cdc42 activation assay and in vitro GDP and GTP loading. HT22 cells were transfected with dTomato-tagged Cdc42 (dTom-Cdc42) and Myc-tagged Par6 (Myc-Par6). For *in vitro* loading, EDTA was added to cell lysates to 20 mM final concentration. The lysates were then incubated with either 1 mM GDP or 100 μM GTPγS with constant agitation at 30°C for 30 min. The reactions were stopped by adding $MgCl_2$ (to 60 mM, final concentration) and used for the subsequent immunoprecipitation procedure.

In vitro *kinase assay.* The activity of PKCζ was assayed by measuring the rate of phosphorylation of the PKCζ-specific peptide substrate (Kazanietz et al., 1993; Nishikawa et al., 1997). Recombinant plasmid of FLAG PKCζ (pCIG2-FLAG PKCζ) was transfected into CGNs and expressed overnight. Cells were serum-starved for 3–5 h and treated with 10 μg/ml NG2 for 10–30 min. After treatment, cells were immediately washed with cold PBS and lysed in 0.3% CHAPS lysis buffer (20 mM phosphate buffer, pH7.4, 150 mM NaCl, 1 mM EDTA, and 0.3% CHAPS) supplemented with proteinase and phosphatase inhibitor cocktail (Roche). The insoluble fraction was removed by centrifugation at 16,000 × *g* for 10 min. One hundred micrograms of lysate were immunoprecipitated with 1 μg of anti-FLAG antibody and 20 μl of protein G bead for 2 h under constant agitation. The beads and immune complexes were centrifuged and washed in 0.3% CHAPS lysis buffer. After three washes, the beads were washed once with and then resuspended in 40 μl of kinase buffer (8 mM MOPS, pH 7.0, 1 mM EDTA), and 2–8 μl of resuspension was diluted in the reaction mixture containing 50 μM peptide substrate and 20 μg/ml phosphatidylserine. The assay mixtures were preincubated at 30°C for 10 min. The reaction was started by adding 5 μCi of γ^{32}P]ATP. After 20 min, 20 μl of assay mixture was spotted onto P81 paper (Millipore Biotechnology) to stop the reaction. The paper was washed three times with 0.75% phosphoric acid for 5 min and once with acetone for 5 min, air dried, and transferred into a scintillation vial. Ten milliliters of scintillation mixture was added to the each vial, and radiation activity was measured in a Beckman LS6500 scintillating counter.

Stripe assay. The stripe assay (Vielmetter et al., 1990) was performed as follows. NG2 (20 μg/ml) or Fc in sterile PBS containing a coloring antibody (goat anti-human-FC-Cy3; Invitrogen) was applied to 100 μm channels of a polydimethylsiloxane (Dow Corning) matrix for 2 h at 37°C on a PLL-coated coverslip. Clustered Ephrin-A5 (10 μg/ml) was printed directly on glass surfaces. After removing the matrix and rinsing with PBS, the patterns were additionally coated with 20 μg/ml laminin for 1 h at 37°C. Retinal strip explants (E7) of 300 μm width were cultivated for 24 h on the patterned coverslips. Afterward, 5 μM Myr-PKCζ-pseudosubstrate peptide (ZIP peptide; Invitrogen), inactivated ZIP peptide (proteinase K treatment at 37° for 30 min followed by heat inactivation at 99° for 15 min), or heat-inactivated proteinase K (99°,15 min) in methylcellulose containing F-12 medium was added for another 12 h. Explant cultures were fixed and stained for laminin and actin. Explant axons covering at least a 1 × 0.8 mm of the patterned surface were analyzed. Image quantification was done with the ImageJ JaCop plug-in for colocalization. The actin signal overlapping the laminin signal was calculated using Manders' coefficient. Data were expressed as the percentage of neurons avoiding the protein of interest.

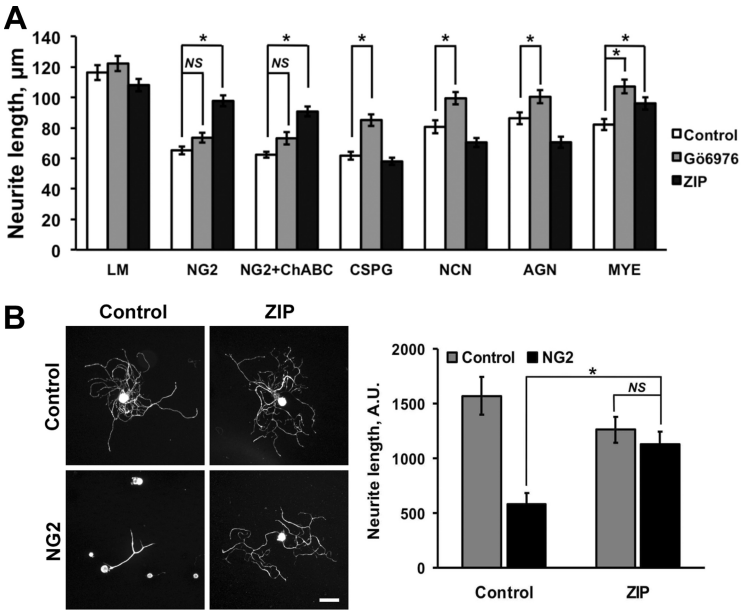

Figure 1. Figure 1.PKCζ is required for axon growth inhibition by NG2. ***A***, The effect of PKC inhibitors on axon growth inhibition by various substrates. Dissociated cerebellar granule neurons were grown on the indicated substrates overnight, and the longest neurite of each cell was measured. The histogram plots the mean neurite lengths ± SEM [~111–304 neurons were counted in each condition; $n = 4$ for the laminin (LM), NG2 CSPG (NG2), and myelin extract (MYE) experiments; $n = 3$ in chick brain CSPG mixture (CSPG), neurocan (NCN), and aggrecan (AGN) experiments; $n = 2$ in the ChABC-treated NG2 experiment (NG2+ChABC); $^*p < 0.001$, Dunn's post test). ***B***, The inhibitory effect of NG2 on axon growth of adult DRG neurons. Dissociated DRG neurons from adult mice were grown either on control substrates or on NG2-coated substrates in the absence or presence of a cell-permeable peptide inhibitor of PKCζ (ZIP peptide, 2 μM). Left, Typical cell fields. Scale bar, 50 μm. The histogram plots the mean neurite lengths ± SEM. Control denotes coverslips coated with laminin. NG2 denotes substrates coated first with 2 μg/ml laminin and subsequently with 10 μg/ml NG2 (>36 cells were counted and scored in each condition; $^*p < 0.001$, Dunn's *post hoc* test). NS, Not significant.

Analysis of neuronal polarity

To quantify the polarization of cells, axons and dendrites were determined by immunostaining; a tau-positive process extending more than twice a cell diameter was defined as an axon. Phalloidin-positive, Tau-negative processes were defined as dendrites. More than 130 cells for each group were examined from three independent experiments.

Statistics

Statistical analysis was performed using SigmaStat software (Systat Software), and either Students' *t* test or Mann–Whitney rank sum test was used. For comparison of multiple data sets with normal distribution, one-way ANOVA was used followed by *post hoc* Tukey's test. For data sets that failed to pass normality test, ANOVA on ranks was used followed by Dunn's post test. Data are presented as mean ± SE, and a value of $p < 0.05$ is considered significant.

Results

To assess the role of PKCζ and the Par complex in axon growth inhibition, we grew postnatal rat CGNs on surfaces coated with either NG2, aggrecan, neurocan, chick brain CSPGs, or rat brain myelin, and treated the cultures with isoform-specific inhibitors of PKC. As shown in Figure 1*A* and consistent with previous studies (Hasegawa et al., 2004; Sivasankaran et al., 2004) Gö6976 [12-(2-cyanoethyl)-6,7,12,13-tetrahydro-13-methyl-5-oxo-5H-indolo(2,3-a)pyrrolo(3,4-c)-carbazole], an inhibitor of conventional PKCs (α and β1) reversed axon growth inhibition caused

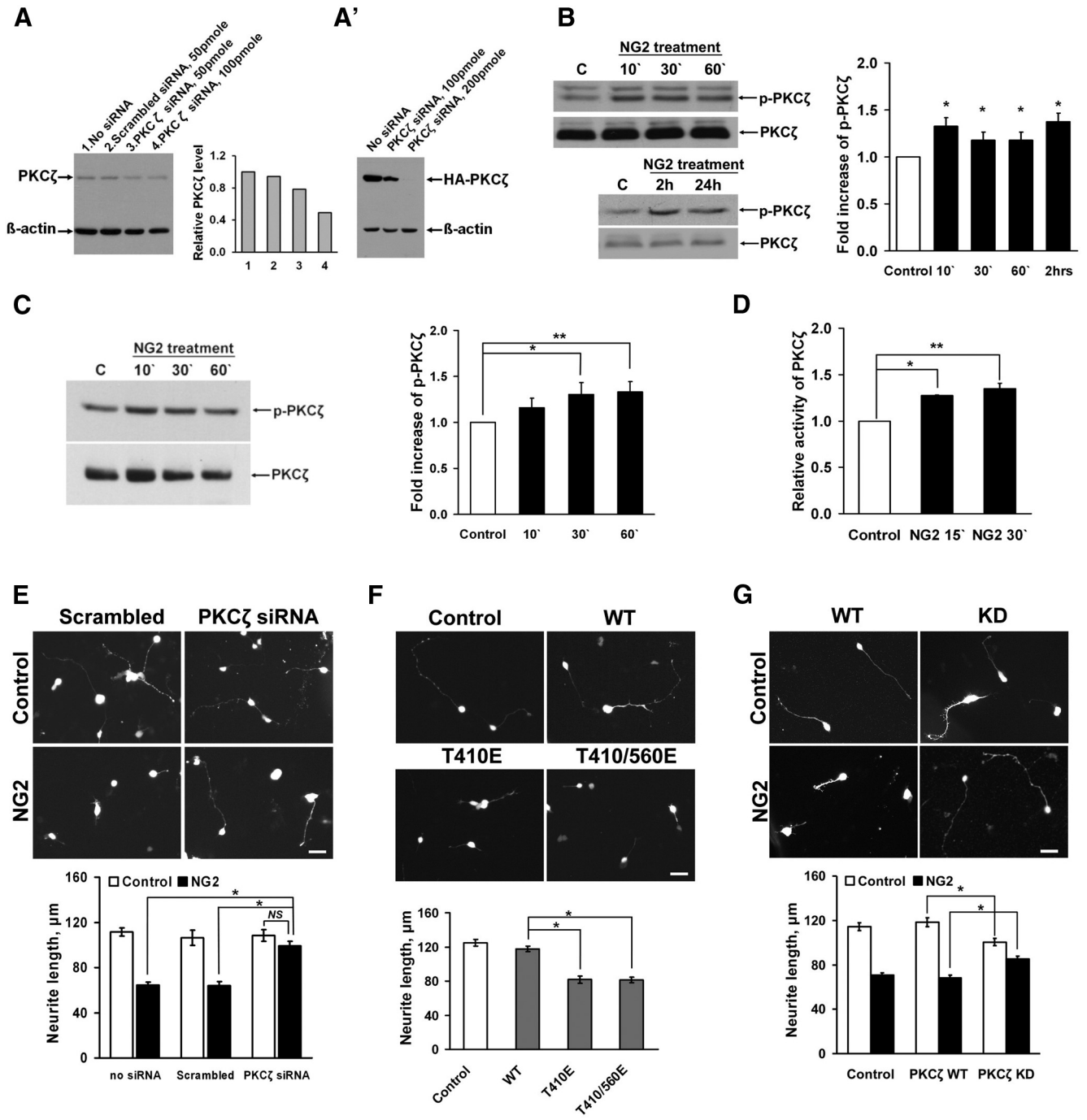

Figure 2. PKCζ is required for axon growth inhibition. ***A***, RNAi-mediated suppression of endogenous PKCζ. Rat CGNs were transfected with the indicated amounts of either scrambled or PKCζ-targeting siRNA. Cell lysates were analyzed by SDS-PAGE and immunoblotting with anti-PKCζ antibody. The histogram shows densitometric quantitation of the PKCζ knockdown. ***A'***, HT22 cells were transfected with HA-PKCζ and the indication siRNAs. The levels of HA-PKCζ in lysates were detected by immunoblotting with anti-HA antibody. ***B***, PKCζ phosphorylated at T410 (p-PKCζ) was detected by immunoblotting with specific anti-phospho-PKCζ antibody. Bath application of soluble NG2 (top) or growth on NG2 coated substrates (bottom) induced the phosphorylation of PKCζ in CGNs. The histogram shows the fold increase in phospho-PKCζ ± SEM relative to control cells after normalization to total PKCζ ($n = 3–6$; *$p < 0.05$, Student's t test). ***C***, PKCζ phosphorylated at Thr410 in HT22 cells was detected by immunoblotting. Bath application of soluble NG2 (10 µg/ml) induced the phosphorylation of PKCζ in HT22 cells. The histogram shows the mean increase in phospho-PKCζ ± SEM [$n = 3$; normalized to control; *not significant (NS); **$p < 0.05$, Students' t test]. ***D***, Rat CGNs were transfected with FLAG-PKCζ, and soluble NG2 (10 µg/ml) was bath applied for the indicated times. PKCζ kinase activity was measured as described in Materials and Methods ($n = 3$; *$p < 0.01$; **$p < 0.05$, Students' t test). ***E***, The effect of PKCζ siRNA on axon growth inhibition. Thirty picomoles of scrambled control or PKCζ-targeted siRNA along with 1.0 µg of dTomato plasmid (pCAGJC-dTomato) were transfected into CGNs. The histogram shows mean neurite lengths ± SEM ($n = 1$ in scrambled siRNA experiment; $n = 3$ in control and PKCζ siRNA experiments; *$p < 0.001$, Dunn's post test). ***F***, The effect of phosphomimetic PKCζ on axon growth. One microgram of indicated PKCζ expression plasmids along with 1 µg of dTomato plasmid were transfected into CGNs. The histogram shows average neurite lengths ± SEM ($n = 3$; *$p < 0.001$, Dunn's post test). ***G***, The effect of kinase-dead (KD) PKCζ in axon growth inhibition. Approximately 1–2 µg of indicated PKCζ expression plasmids along with 1 µg of dTomato plasmid was transfected into CGNs. For the histogram, $n = 3$. *$p < 0.005$ (Dunn's post test). Scale bars: 50 µm.

by myelin, mixed chick brain CSPGs, pure neurocan, and aggrecan, but did not reverse inhibition induced by either the ECD of the NG2 proteoglycan (Ughrin et al., 2003) or the ECD after treatment with chondroitinase ABC to remove any covalently attached glycosaminoglycan (GAG) chains. Neither the chick brain CSPG mixture nor myelin membrane preparation contained detectable NG2 (S. Lee and J. Levine, unpublished observation). A broad range inhibitor of PKC (calphostin C) partially restored neurite growth on NG2-coated surfaces (data not shown), suggesting that additional isoforms of PKC may be involved in growth inhibition. We therefore grew neurons in the presence of a cell-permeable pseudosubstrate peptide inhibitor of atypical PKCζ (referred to herein as ZIP peptide). Addition of the ZIP peptide (2 μM) reversed the growth inhibitory activity of both NG2-coated and myelin-coated substrates but had no effect on inhibition induced by either mixed chick brain CSPGs or the purified CSPGs (Fig. 1*A*). NG2 also inhibits the growth of DRG neurons (Dou and Levine, 1994), and the ZIP peptide restored normal neurite length to adult mouse DRGs grown on NG2-coated surfaces (Fig. 1*B*). These data suggest a role for PKCζ in NG2 and myelin-induced growth inhibition. Because myelin membranes contain multiple inhibitors of neurite outgrowth that can activate different intracellular signaling pathways (Schwab et al., 2005), we used purified recombinant NG2 ECD in the following studies to analyze the specific role of PKCζ in the regulation of axon growth.

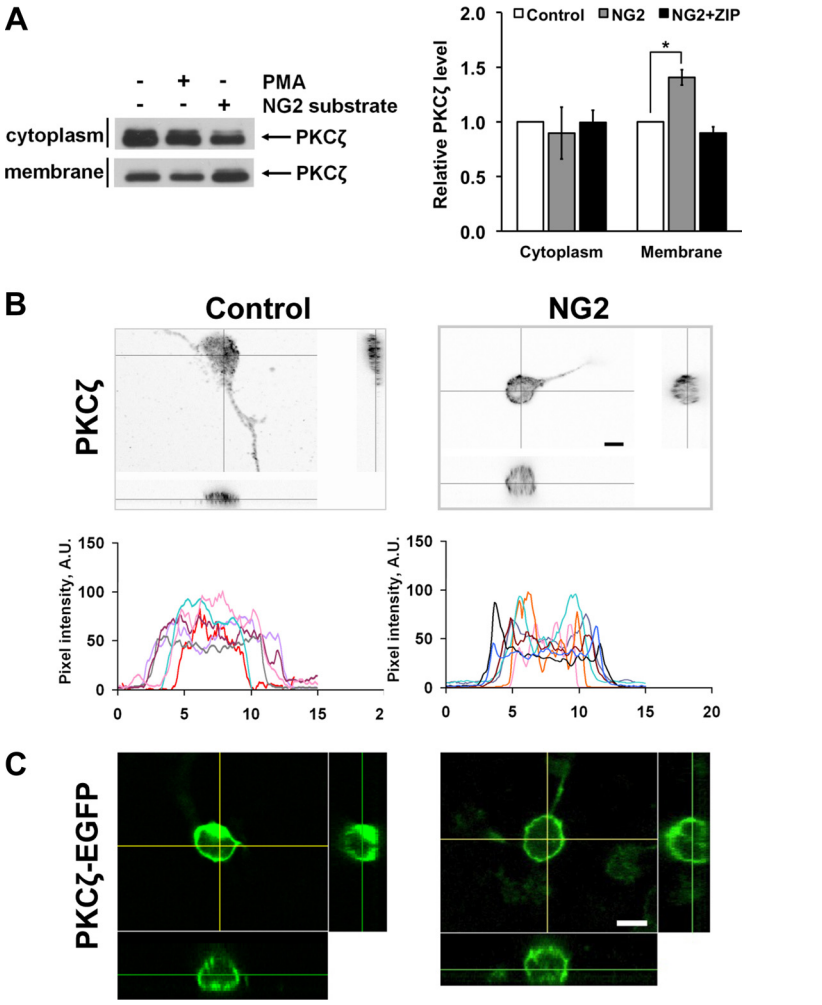

Figure 3. Enrichment of PKCζ in membrane fractions induced by NG2 treatment. ***A***, CGNs were grown overnight on control or NG2-coated dishes. After cell lysis, cytoplasmic and membrane fractions were prepared as described in Materials and Methods, and PKCζ in each fraction was detected by SDS-PAGE followed by immunoblotting with anti-PKCζ. Treatment of the cells with PMA had no effect on the compartmentalization of PKCζ. The histogram shows fold changes in PKCζ levels in cytoplasmic and membrane fractions after NG2 treatment ($n = 3$). Addition of ZIP peptide prevented the increase in membrane-associated PKCζ ($n = 2$). $^*p < 0.05$, Student's *t* test. ***B***, NG2 treatment translocates PKCζ to the membrane. Rat CGNs were plated on the surfaces coated either with laminin only or with laminin plus NG2, grown for 24 h, and fixed and stained with anti-PKCζ antibody. The top panel shows strong PKCζ immunoreactivity associated with the membrane of cells grown on the NG2-coated substrate. Shown below are line scans of fluorescence intensity through the cell bodies ($n = 6$). ***C***, Rat CGNs transfected with GFP-tagged PKCζ were grown on either control or NG2-coated substrates for 24 h. The distribution of fluorescence was analyzed using confocal microscopy. Fluorescence was condensed at the membrane of cells grown on NG2. Scale bars: 10 μm.

NG2 activates PKCζ

To explore the role of PKCζ, we used siRNA to knock-down PKCζ expression. As shown in Figure 2*A*, transfection of CGNs with a siRNA pool directed against PKCζ was effective in reducing PKCζ levels. Western blots of bulk-transfected cultures likely underestimate the extent of knock-down since the transfection efficiency of CGNs was ~30–40%. PKCζ-targeted siRNA also reduced effectively the expression of HA-tagged PKCζ in transfected HT22 cells, a neural cell line (Fig. 2*A′*). Transfection of CGNs with PKCζ siRNA but not control scrambled siRNA restored normal neurite growth on NG2-coated surfaces (Fig. 2*E*). This requirement for PKCζ suggests that the enzyme may be activated by NG2 treatment. PKCζ activation is a two-step process: phosphorylation of T410 releases the kinase from inhibition allowing autophosphorylation of T560 and full activation (Chou et al., 1998; Standaert et al., 2001). We measured the phosphorylation of T410 on immunoblots as an indication of the activation of PKCζ by NG2. Short-term treatment of CGNs with soluble NG2 led to a modest but significant increase in the phosphorylation of T410. This increase was sustained for as long as 24 h when the cells were grown on NG2-coated surfaces (Fig. 2*B*). To measure kinase activity directly, we developed an *in vitro* kinase activity assay using HT22 cells. Similar to CGNs, HT22 cells respond to short-term treatment with soluble NG2 with an increase in T410 phosphorylation (Fig. 2*C*). To avoid assaying the activation of conventional or novel PKCs, we designed an assay to measure specifically PKCζ activity. Cells were transfected with FLAG-tagged PKCζ, the kinase was then immunoprecipitated with anti-Flag antibodies, and the immunoprecipitates were incubated with ^{32}Pγ-ATP and peptide substrates and inhibitors specific for either conventional, novel, or atypical PKCs. PKCζ activity is defined as cpms incorporated into the atypical PKC peptide substrate minus cpms incorporated in the presence of ZIP peptide. In this assay, Gö6976 had no effect on specific PKCζ activity. Short-term treatment of transfected rat CGNs resulted in an increase in PKCζ activity (Fig. 1*D*). To determine whether the phosphorylation and activation of PKCζ is sufficient to inhibit axon growth from

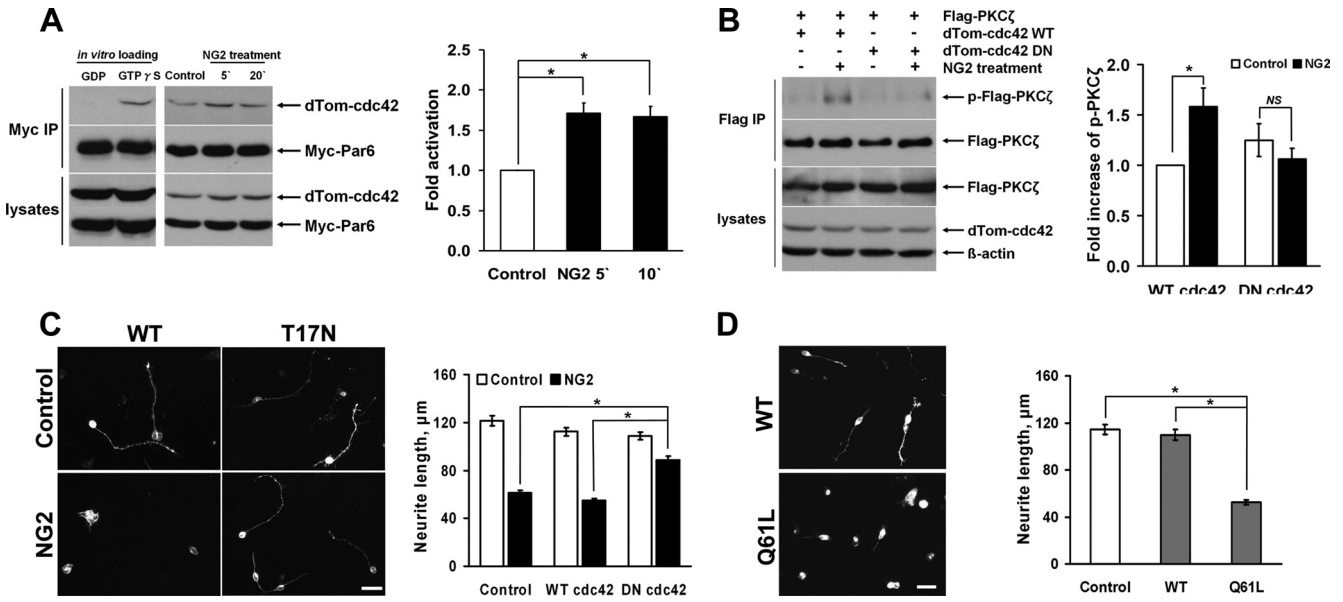

Figure 4. A Cdc42-Par6 complex is required for axon growth inhibition. ***A***, NG2 activates Cdc42. HT22 cells were transfected with dTom-Cdc42 and Myc-Par6. For *in vitro* loading, cell lysates were incubated with either GDP or GTPγS as described in Materials and Methods. The cells were treated with soluble NG2 (35 μg/ml) for the indicated times, and the interaction of cdc42 and Par6 was measured by immunoprecipitation with anti-myc-tag antibody, followed by immunoblotting with either anti-dsRed or anti-myc antibody. The histogram shows the mean ± SEM ($n = 3$, normalized to control treatment; $^*p < 0.05$, Student's *t* test). ***B***, DN-Cdc42 prevents the NG2-induced phosphorylation of PKCζ. NG2 (10 μg/ml) was bath applied for 30 min to HT22 cells transfected with either WT or DN forms of Cdc42 along with FLAG-PKCζ. The phosphorylation of PKCζ was detected by immunoprecipitation with anti-FLAG antibody and by immunoblotting with specific anti-phospho-PKCζ antibody. The histogram shows the fold increase in PKCζ phosphorylation (mean ± SEM; $n = 3$, normalized to the control treatment of WT-Cdc42-transfected cells; $^*p < 0.05$, Student's *t* test). ***C***, DN-Cdc42 restores normal neurite growth. CGNs were transfected with either WT or DN-Cdc42 (T17N) expression plasmids and grown on either control or NG2-coated substrates. The histogram shows mean neurite lengths ± SEM ($n = 3$; $^*p < 0.001$; Dunn's post test). ***D***, CA-Cdc42 inhibits neurite growth. CGNs were transfected with CA-Cdc42 (Q61L) and grown and measured as in ***C***. The histogram plots mean neurite lengths ($n = 3$; $^*p < 0.001$, Dunn's post test). NS, Not significant. Scale bars: 50 μm.

rat CGNs, we created two phosphomimetic forms of PKCζ by converting T410 and T560 to glutamic acid (Chou et al., 1998; Standaert et al., 2001). Expression of either T410E or both T410E and T560E reduced significantly axon lengths on laminin-coated substrates (Fig. 2*F*). CGNs transfected with a kinase-dead mutant of PKCζ (Romanelli et al., 1999) were not growth-inhibited on NG2 substrates, whereas transfection with wild-type PKCζ had no effect on NG2-induced growth inhibition (Fig. 2*G*). When activated, PKC isoforms are translocated from a cytoplasmic compartment to the plasma membrane (Mosthaf et al., 1996; Standaert et al., 1999; Kazi and Soh, 2007). We therefore measured changes in the amount of PKCζ associated with cytoplasmic or membrane fractions of rat CGNs grown on either control laminin alone or NG2 plus laminin-coated surfaces for 24 h. As shown in Figure 3*A*, there was a significant increase in the amount of PKCζ associated with the plasma membrane and a decrease in the cytoplasmic pool of PKCζ after growth on NG2. Short-term treatment of the cultures with PMA had no effect on the compartmentalization of PKCζ, whereas addition of the ZIP peptide (2 μM) 3 h before lysis prevented this increase in membrane association. Last, we grew CGNs on either laminin-coated surfaces or surfaces coated with laminin and NG2 for 24 h and immunofluorescently stained the cells with antibodies against PKCζ. The distribution of PKCζ was analyzed using confocal microscopy. As shown in Figure 3*B*, there was an increase in the association of endogenous PKCζ with the plasma membrane. In cells transfected to express EGFP-PKCζ, there was also an increase in membrane-associated fluorescence after plating on NG2-coated surfaces (Fig. 3*C*). Thus, by three different criteria, treatment of rat CGNs with soluble or substrate-bound NG2 activates PKCζ, and this activation is both necessary and sufficient to inhibit axon elongation.

NG2 activates Cdc42 and the Par complex

PKCζ is a component of the Par complex that is usually associated with the development of neuronal polarity rather than the regulation of axon elongation. During axonogenesis, Cdc42 binds to and activates Par6. Par6 normally inhibits PKCζ, but after Cdc42 binding, PKC becomes disinhibited (Lin et al., 2000; Etienne-Manneville and Hall, 2001; Yamanaka et al., 2001; Macara, 2004; Hurd and Margolis, 2005; Nishimura et al., 2005). The complex of PKCζ, Par6, and Par3 is subsequently transported to the ends of differentiating axons where it induces growth cone formation and axon elongation (Shi et al., 2003; Nishimura et al., 2004). Since the functions of the Par complex can vary according to cellular context and protein–protein interactions (Wang et al., 2003; Ozdamar et al., 2005; Nakayama et al., 2008; Zhang and Macara, 2008; Yi et al., 2010), we performed a series of experiments to determine the roles of Cdc42 and Par6 in the activation of PKCζ by NG2 and to ask whether, once activated by NG2, there are changes in Par complex stoichiometry, localization, and/or function.

We measured changes in the association of Par6 and Cdc42 as an assay for Cdc42 activation by exogenous NG2. To confirm that the increased binding of Cdc42 to Par6 is a measure of Cdc42 activation, HT22 cells were transfected with dTomato-tagged Cdc42 and myc-tagged Par6, and the amount of Cdc42 bound to Par6 was measured from immunoblots after immunoprecipitation of Par6. As shown in Figure 4*A*, incubation of transfected cell lysates with GTPγS but not GDP increased the binding of Cdc42 to Par6. Treatment of transfected HT22 cells with soluble NG2 for 5 and 20 min increased the binding of Cdc42 to Par6 (Fig. 4*A*). To determine whether the activation of Cdc42 is required for the NG2-induced increases in PKCζ phosphorylation, we transfected

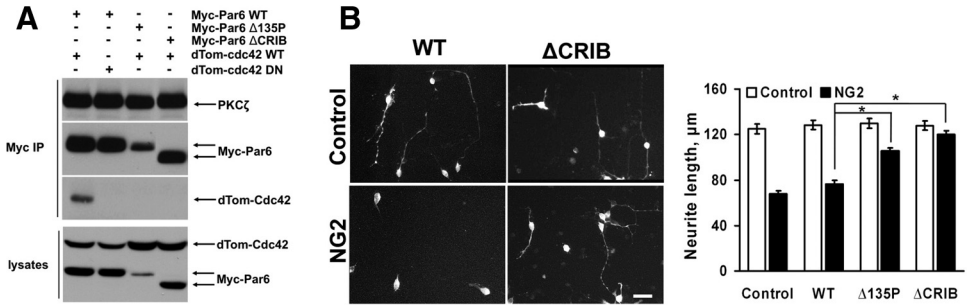

Figure 5. The semi-CRIB domain of Par6 is required for the binding of Cdc42 and neurite growth inhibition. ***A***, HT22 cells were cotransfected with the indicated forms of Par6 and Cdc42. After 16–24 h, cell lysates were immunoprecipitated by anti-Myc antibody and blotted with antibodies against Myc, FLAG, and PKCζ. Semi-CRIB domain mutants failed to bind to Cdc42, whereas they are still able to associate with PKCζ. ***B***, A Par6-Cdc42 interaction is necessary for growth inhibition. CGNs were transfected with Par6 mutants (Δ135P and ΔCRIB), and neurite lengths were measured as above ($n = 3$; $^*p < 0.001$, Dunn's post test). Scale bar, 50 μm.

HT22 cells with either wild-type or DN Cdc42 (T17N) and measured the phosphorylation of T410 in FLAG-tagged PKCζ. Expression of DN-Cdc42 prevented NG2-induced increases in T410 phosphorylation (Fig. 4*B*). Wild-type Cdc42 bound strongly to Par6, whereas the dominant-negative form did not (Fig. 5*A*). We next examined the effects of manipulating Cdc42 activity on axon growth from CGNs. Transfection of CGNs with DN-Cdc42 reversed growth inhibition on NG2-coated surfaces (Fig. 4*C*), whereas transfection with a CA mutant of Cdc42 (Q61L) was sufficient to inhibit neurite outgrowth on control laminin-only substrates (Fig. 4*D*). Thus, NG2 treatment activates Cdc42, and this activation is necessary for both the activation of PKCζ and for NG2-induced axon growth inhibition. CA-Cdc42 is sufficient to inhibit neurite outgrowth on control laminin-coated substrates.

To determine whether the increased association of Par6 and active Cdc42 is necessary for axon growth inhibition, we transfected cells with two mutant forms of Par6 lacking the semi-CRIB domain that binds to activated Cdc42 (Lin et al., 2000; Nishimura et al., 2005). Wild-type Par6 forms complexes with Cdc42 *in vivo*, but these mutants do not. All forms of Par6, however, are bound to PKCζ (Fig. 5*A*). When transfected into CGNs, these mutant forms of Par6 significantly reversed NG2-induced growth inhibition (Fig. 5*B*). Together, these data show that NG2 treatment activates Cdc42 and increases its association with Par6, and both the activation and increased association are necessary for axon growth inhibition.

We next asked whether NG2 treatment changes the association of PKCζ and Par6. As shown in Figure 6*A*, NG2 treatment increased the amount of Par6 associated with PKCζ in both transfected HT22 cells and CGNs. PKCζ and Par6 associate via their N-terminal PB1 domains (Gao et al., 2002; Nishimura et al., 2005). To disrupt the increased Par6–PKCζ binding, we transfected CGNs with an N-terminal fragment of PKCζ (residues

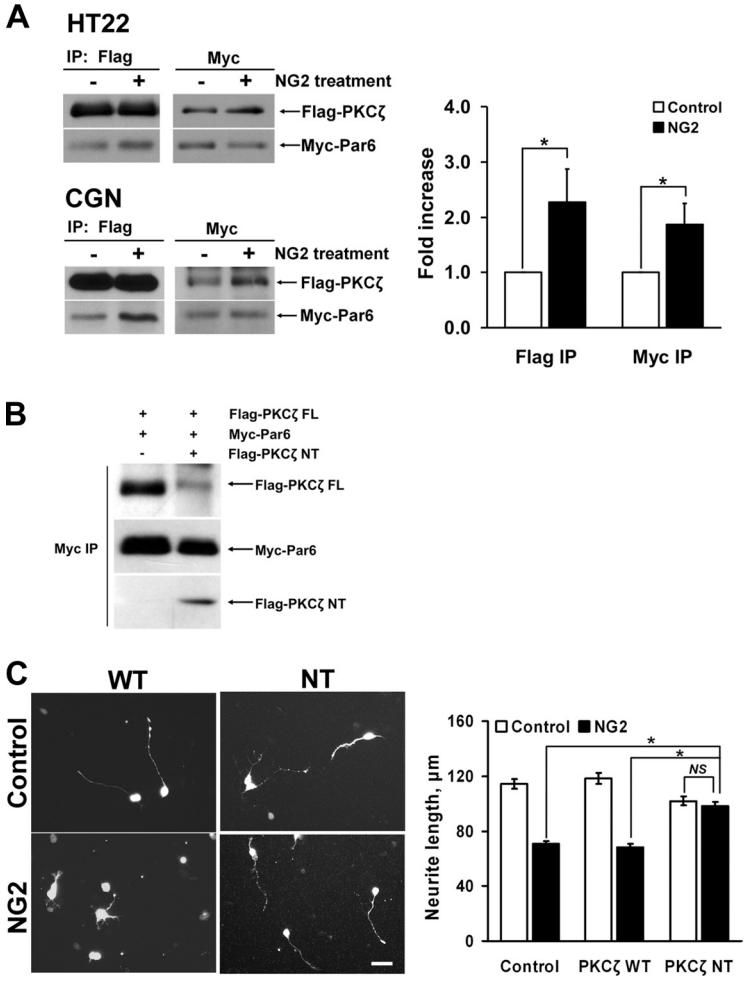

Figure 6. A PKCζ–Par6 complex is required for NG2-induced growth inhibition. ***A***, NG2 treatment increases the association of PKCζ with Par6. CGNs and HT22 cells were transfected with FLAG-PKCζ and Myc-Par6, and NG2 (10 μg/ml) was bath-applied to the rat CGNs for 15 min or to the HT22 cells for 30 min. The association of these epitope-tagged proteins was detected by immunoprecipitation followed by immunoblotting with epitope-specific antibodies. The histogram to the right plots fold increase in Par6–PKCζ binding in HT22 cells (mean ± SEM; $n = 3$; $^*p < 0.05$, Student's *t* test. ***B***, HT22 cells were cotransfected with Par6 and PKCζ PB1 domain-expressing plasmid (NT). After 16–24 h, cell lysates were immunoprecipitated by anti-Myc antibody and blotted with antibodies against Myc and FLAG. PKCζ PB1 domain mutants prevented the interaction of PKCζ and Par6. ***C***, CGNs were transfected with PKCζ PB1 domain-expressing plasmid (NT) and grown on control or NG2-coated substrates. The histograms shows mean neurite lengths ± SEM ($n = 3$; $^*p < 0.001$, Dunn's post test). NS, Not significant. Scale bar, 50 μm.

1–129, PKCζ NT) that competes for Par6 binding and grew the cells on control or NG2-coated surfaces. The expression of PKCζ NT reduces the association of PKCζ and Par6 in CGNS (Fig. 6*B*) and reverses NG2-induced axon growth inhibition (Fig. 6*C*). Expression of WT PKCζ had no effect on NG2-induced inhibition. Together, these results show NG2 treatment of CGNs activates the Par complex and this activation is necessary for growth inhibition.

Atypical PKC and the Par complex regulate the development of polarity in embryonic hippocampal neurons (Shi et al., 2003; Nishimura et al., 2005). Inhibition of PKCζ prevents polarization (Shi et al., 2003), and activation of the kinase promotes polarization and axonogenesis (Zhang et al., 2007). Enhancing the activity of PKCζ can lead to aberrant polarization and the formation of multiple axons per cell (Zhang et al., 2007). To confirm a functional activation of PKCζ by NG2 in a system other than postnatal CGNs, we asked whether substrate-bound NG2 could affect the polarization of embryonic day 18 rat hippocampal neurons. We grew the cells on surfaces coated with either PLL or PLL and NG2, and measured the number of cells with and without axons. As shown in Figure 7*A*, hippocampal neurons grown on NG2-coated surfaces rapidly extended Tau-positive axonal processes, such that after 48 h in culture, a higher percentage of the cells had one or more axons. This percentage was reduced to control levels when the cells were grown on NG2 in the presence of 2 μM ZIP peptide. Typical cells (48 h in culture) stained with phalloidin and anti-Tau antibodies are also shown in Figure 7*A*. The control cell has one long axonal process and several short processes emanating from the cell body and corresponds to stage 3/4 of polarization (Dotti et al., 1988). The cell grown on NG2 has four long Tau-positive axonal processes. Thus, NG2 treatment perturbs the development of polarity in embryonic hippocampal neurons, and this perturbation is dependent on PKCζ activity.

NG2, as well as other CSPGs, form barriers that growing and sprouting axons avoid *in vitro* and *in vivo* (Snow et al., 1990; Dou and Levine, 1994; Powell et al., 1997; Asher et al., 2000; Tan et al., 2006). We reasoned that if the inhibitory effect of NG2 on growing axons is via an activation of PKCζ, manipulating PKCζ should also alter axonal behavior in barrier assays such as the widely used stripe assay (Vielmetter et al., 1990). As shown in Figure 7*B*, axons of embryonic chicken retinal ganglion cells avoid NG2 to an extent similar to the avoidance of ephrin-A5 in the stripe assay. This avoidance of NG2 stripes was reduced by addition of ZIP peptide, whereas the avoidance of ephrin-A stripe was not affected. Pretreating the ZIP peptide with proteinase K to cleave and inactivate it restored avoidance of NG2 stripes. Heat-inactivated proteinase K had no effect on axon growth in this assay. Since the retinal ganglion cells shown here have already polarized and are actively extending axons, these data demonstrate that growth cone contact with NG2 causes the repulsion of actively growing axons, and that this repulsion requires the activation of PKCζ.

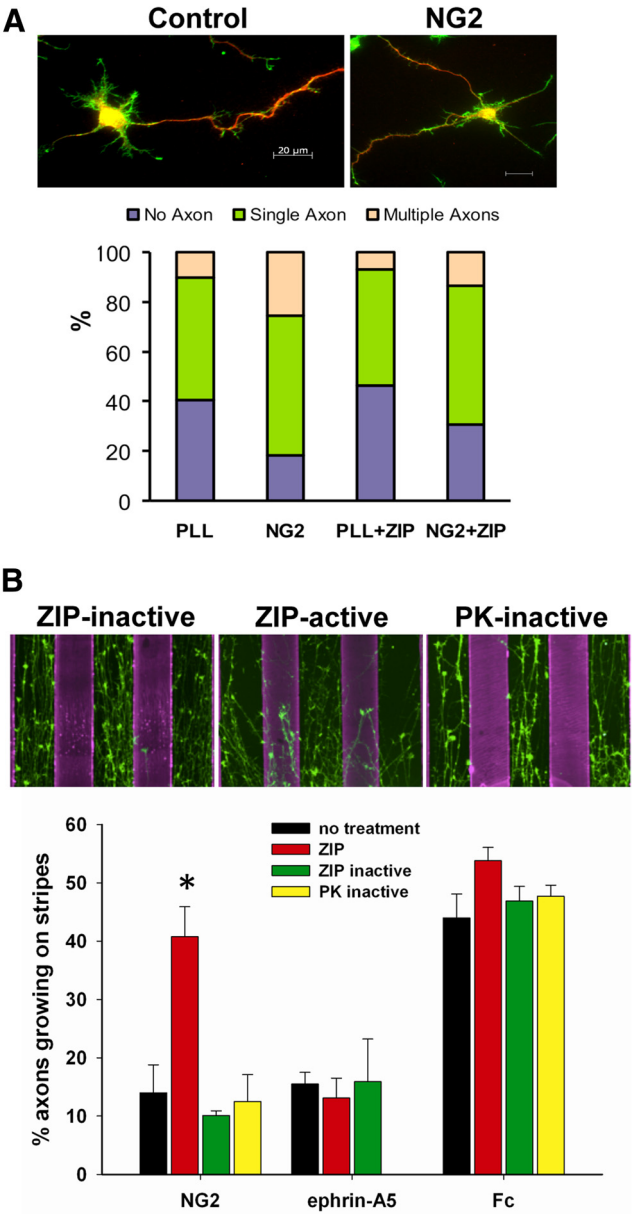

Figure 7. ***A***, NG2 promotes axon formation in hippocampal neurons. E18 hippocampal neurons were grown on PLL- or NG2-coated surfaces for 24–48 h and cell polarization analyzed as described in Materials and Methods. The bar graph shows the percentage of neurons with the indicated number of axons ($n = 3$; >136 cells were counted and scored in each condition). The panels below show a typical stage 3/4 cell on control substrate and a multiaxonal cell grown on NG2 immunofluorescently stained with anti-Tau antibodies (red) and Alexa Fluor 488 phalloidin (green). Scale bar, 20 μm. ***B***, The avoidance of NG2 in the stripe assay requires PKCζ activity. E7 chick retina was grown on striped surfaces coated with NG2 (purple), and living cultures were treated as indicated. The histogram below plots the percentage of neurites growing on the stripes. PK, Proteinase K. *$p < 0.001$. $n = 4–6$ for each condition.

NG2 treatment activates Rac1 GTPase

How does the activation of PKCζ and the Par complex lead to reduced axon extension? Most of the effects of the Par complex on the cytoskeleton and cell motility are mediated through Par3 which plays a central role in regulating Rac1 activity (Chen and Macara, 2005; Nishimura et al., 2005; Nakayama et al., 2008). Since Par3 may function independently from any associations with other Par complex proteins (Chen and Macara, 2005), we first examined the associations of PKCζ with Par3. Treatment of transfected HT22 cells or CGNs with NG2 reduced the amount of Par3 coimmunoprecipitated with PKCζ (Fig. 8*A*). There was also less PKCζ present in anti-Par3 immunoprecipitates. This NG2-dependent reduction in the interactions of Par3 and PKCζ was prevented by either transfecting cells with a kinase-dead mutant of PKCζ or treating the cells with ZIP peptide (Fig. 8*B*). Treatment of cells with the Rho kinase (ROCK) inhibitor Y27632 [(R)-(+)-*trans*-N-(4-Pyridyl)-4-(1-aminoethyl)-cyclohexanecarboxamide, 2HCl] did not prevent the NG2-induced reduction in Par3–PKCζ binding, suggesting that Rho plays little or no role in either the NG2-

dependent activation of PKCζ or in regulating its protein–protein interactions.

The binding of Par3 and PKCζ is regulated by multiple phosphorylations of Par3. Phosphorylation of T833 by ROCK or S827 by atypical PKC reduces Par3–PKCζ binding (Nagai-Tamai et al., 2002; Nakayama et al., 2008). Because inhibiting ROCK had no effect on the reduced PKCζ–Par3 binding caused by NG2, we mutated S824 of human Par3 (the equivalent of rat Par3 S827) to alanine and tested the effects of this mutation on NG2-induced growth inhibition. Expression of phosphomutant Par3 was able to reverse NG2-mediated neurite growth inhibition (Fig. 8*C*), suggesting that PKCζ-mediated phosphorylation of Par3 is necessary for growth inhibition.

We next asked whether NG2 treatment activates Rac1. To measure the activation of Rac1, we designed a second *in vivo* assay: we transfected cells with myc-tagged pak1 and dTomato-tagged Rac1 and measured the binding of Rac1 to pak1 by immunoprecipitation and immunoblotting. As shown in Figure 9*A*, short-term treatment with NG2 increased the binding of Rac1 to pak1, and this was prevented by the ZIP peptide or expressing phosphomutant Par3 (S824A). To determine the role of Rac1 in neurite growth inhibition, we transfected cells with DN (T17N) or CA-Rac1(G12V). Expression of DN-Rac1 prevented NG2-induced neurite growth inhibition (Fig. 9*B*), and expression of a CA-Rac1 mutant was sufficient to inhibit neurite growth on control laminin-coated surfaces (Fig. 9*C*).

Last, we asked whether NG2 treatment altered the intracellular distribution of Par3. In CGNs grown on control surfaces, Par3 was found in the cell body, axon shaft, and growth cone (Fig. 10). After growth on NG2-coated surfaces for 24 h, the relative amount of Par3 immunoreactivity in the cell body increased, whereas immunoreactivity in axon shafts was reduced. Together, these data suggest a model in which NG2 binding to an unidentified receptor on CGNs (Dou and Levine, 1997) leads to the activation of Cdc42. This increases the binding of Par6 to PKCζ and activates (or disinhibits) the enzyme. PKCζ phosphorylates Par3 at S827, releasing it from PKCζ. Par3 then accumulates in cell bodies leading to the spatially inappropriate activation of Rac1 GTPase and reduced neurite growth.

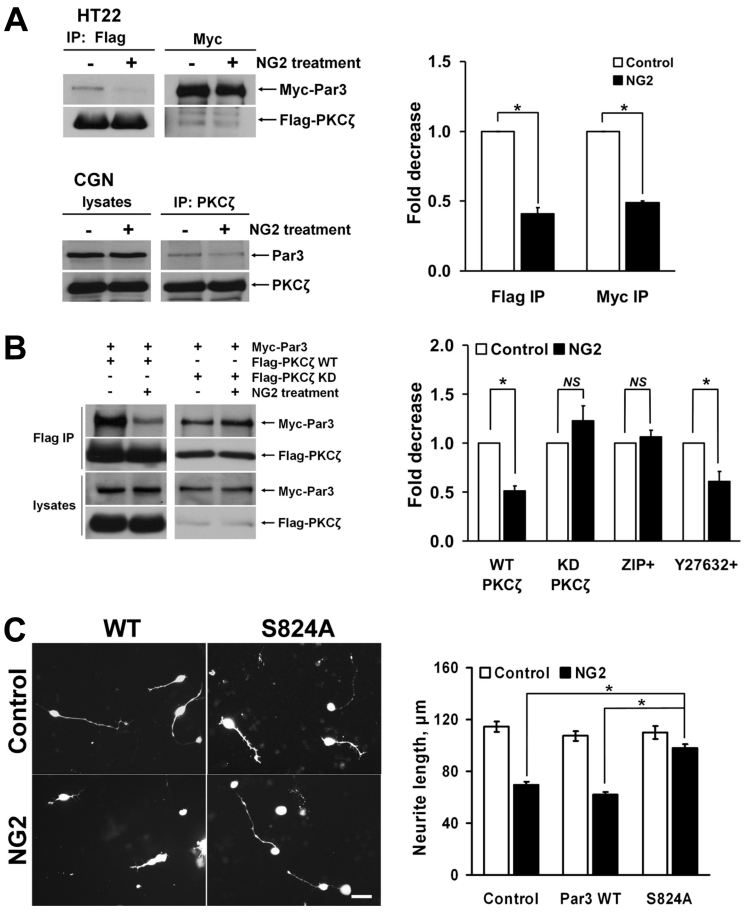

Figure 8. The modification of a PKCζ–Par3 complex by NG2. ***A***, NG2 treatment dissociates a PKCζ–Par3 complex. NG2 (10 μg/ml) was bath applied for 30 min to HT22 cells and CGNs transfected with FLAG-PKCζ and myc-Par3. The binding of these proteins was detected by immunoprecipitation followed by immunoblotting with epitope-specific antibodies. The histogram to the right shows the mean ± SEM decrease in Par3–PKCζ binding in HT22 cells ($n = 3$, normalized to control; $^*p < 0.05$, Student's *t* test). ***B***, PKCζ activity is required for the dissociation of the PKCζ–Par3 complex. NG2 (10 μg/ml) was applied for 30 min to HT22 cells transfected with Par3 and either WT or kinase-dead (KD) forms of FLAG-PKCζ in the absence or presence of ZIP peptide (2 μM) or Y27632 (10 μM). The PKCζ–Par3 complex was detected by immunoprecipitation with anti-FLAG antibody, followed by immunoblotting with specific anti-myc or FLAG antibody. Quantitation of the results is shown to the right ($n = 3$, normalized to control treatment; $^*p < 0.05$, Student's *t* test). ***C***, Expression of a phosphorylation-deficient mutant Par3 (S824A) prevents axon growth inhibition. CGNs were transfected with either WT or phosphorylation-deficient Par3 and grown on control or NG2-coated substrates. The histogram shows the quantitation of neurite lengths (mean ± SEM; $n = 3$; $^*p < 0.001$; Dunn's post test). NS, Not significant. Scale bar, 50 μm.

Discussion

Here, we have shown that atypical PKCζ function is required for axon growth inhibition caused by exposing both neonatal and adult neurons to the extracellular domain of the NG2 CSPG. PKCζ activity, along with that of other isoforms of PKC, is also involved in growth inhibition by myelin membranes (Hasegawa et al., 2004, Sivasankaran et al., 2004). Although PKCζ can have kinase activity-independent functions (Kim et al., 2009), short- and long-term exposure to NG2 activates PKCζ, and this activation is both necessary and sufficient for axon growth inhibition. This activation of PKCζ leads to changes in the function and location of Par complex proteins and the activation of Rac1. Thus, in addition to regulating axon specification, the Par complex regulates axon extension, and this regulation can be negatively modified by extracellular signals. These results define a new role for the Par complex and suggest that the Par complex and PKCζ may be important targets for interventions designed to encourage axon regeneration after injury.

In developing hippocampal neurons, a consequence of PKCζ activation by exogenous NG2 is aberrant polarization and axonogenesis, including the development of multiple axons per cell. This ability of NG2 to promote axonogenesis in embryonic neurons may be why others (Yang et al., 2006b; Busch et al., 2010) concluded that NG2 can be a favorable substrate for growing axons. In neonatal and adult neurons, however, NG2-induced activation of PKCζ reduces axon extension. This suggests that the effects of activation of PKCζ vary according to cell type, developmental stage, and *in vitro* context and likely reflects different

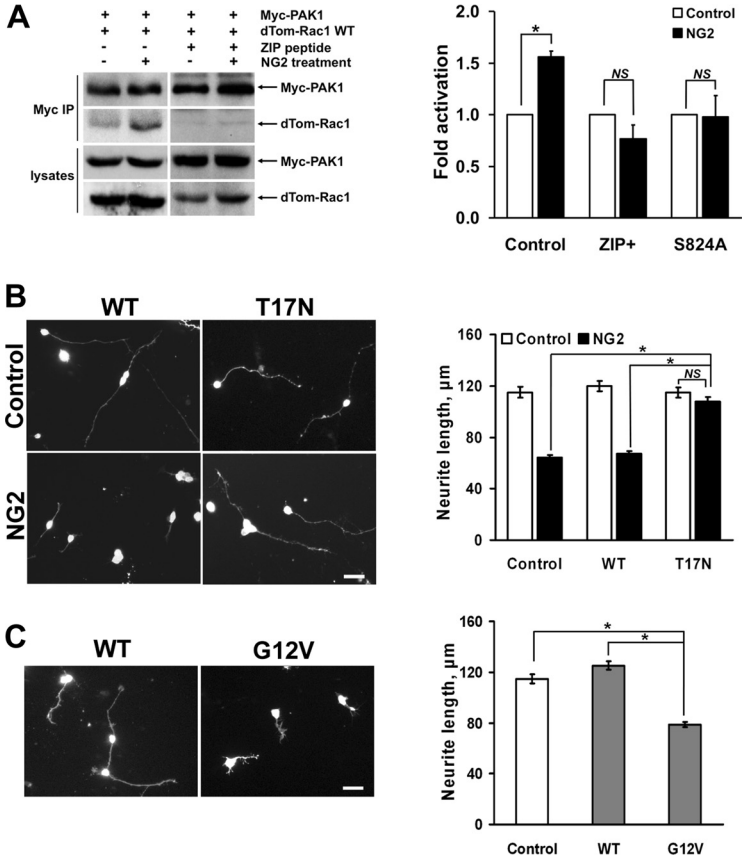

Figure 9. NG2 activates Rac1 to inhibit axon growth. ***A***, NG2 was bath applied for 5 min to HT22 cells transfected with epitope-tagged PAK1 and Rac1 in the absence or presence of ZIP peptide (2 μM) for 5 min. Rac1 binding to transfected PAK1was measured by immunoprecipitation with anti-myc antibody followed by immunoblotting with anti-dsRed. The histogram to the right shows that NG2 increased Rac1 binding to PAK1, and this was prevented either by adding ZIP peptide or expressing the phosphorylation-deficient mutant form of Par3 ($n = 3$, normalized to control; $^*p < 0.05$, Student's *t* test). ***B***, Rac1 activation is required for axon growth inhibition. CGNs were transfected with either WT or DN-Rac1 (T17N) and grown on control or NG2-coated substrates. DN-rac1-expressing CGNs were able to extend long axons on NG2 substrates, similar to the cells grown on control substrates. The histogram shows mean neurite lengths ± SEM ($n = 3$; $^*p < 0.001$, Dunn's post test). ***C***, Constitutively active Rac1 is sufficient to inhibit axon growth from CGNs. WT or CA-Rac1 (G12V) was transfected into CGNs. CA-Rac1-expressing CGNs extended only short stubby axons on control substrates. The histogram shows mean neurite lengths ± SEM ($n = 3$; $^*p < 0.001$; Dunn's post test). Scale bars: 50 μm.

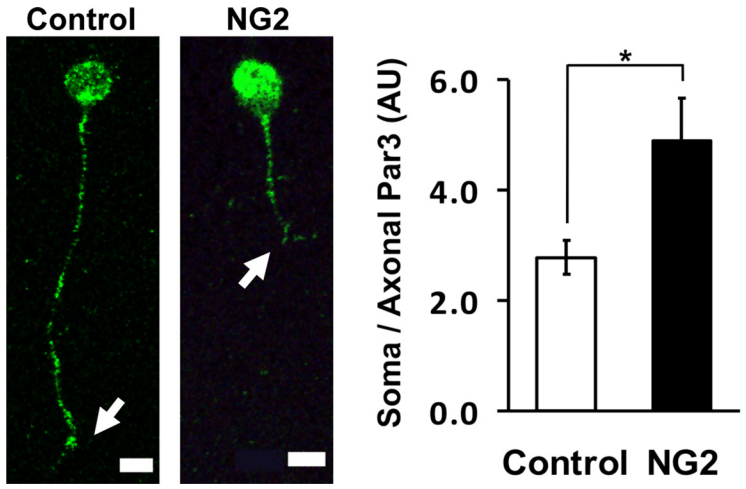

Figure 10. NG2 treatment alters the spatial distribution of Par3 in CGNs. CGNs were grown on either control or NG2 substrate for 24 h and stained with anti-Par3 antibody. Arrows point to the growth cones. The histogram shows the average ratio of Par3 fluorescence in the cell body to that of the axonal compartment (mean ± SEM; $n = 15$ for each condition; $^*p < 0.05$, Student's *t* test). Scale bars: 10 μm.

functions for the Par complex at different stages of neuronal differentiation. In addition to its effects on neonatal CGNs and adult DRGs, NG2 repels chick retinal ganglion cell growth cones in the stripe assay, also in a PKCζ-dependent manner. Growing neurons on uniformly coated substrates measures the ability of substrate molecules to affect axon extension, whereas the stripe assay measures decision making by growth cones. This assay may better reflect axonal behavior after injury *in vivo*, where a growth cone confronts a myriad of growth-promoting and growth-inhibiting molecules.

During the intrinsic polarization of hippocampal neurons, there is a requirement for the activation of Cdc42, which subsequently binds to Par6, resulting in the disinhibition of PKCζ (Lin et al., 2000; Etienne-Manneville and Hall, 2001; Yamanaka et al., 2001; Macara, 2004; Hurd and Margolis, 2005). The inhibition of axon growth by exogenous NG2 also required Cdc42. Because of the low level of Cdc42 expression in CGNs and the liability of bound GTP in cell lysates, we developed a novel *in vivo* Par6 binding assay to demonstrate that Cdc42 is activated after short-term treatment with NG2. Cdc42 activation is required for NG2 effects on growing axons since the expression of DN-Cdc42 reversed axon growth inhibition and prevented the activation of PKCζ. Moreover, expression of CA-Cdc42 inhibited neurite growth of CGNs on laminin surfaces as it also does for embryonic hippocampal neurons (Nishimura et al., 2005). The expression of DN-Cdc42 promotes neurite growth on collapsin-1 (semaphorin 3D)-coated surfaces (Jin and Strittmatter, 1997; Kuhn et al., 1999), suggesting that other growth inhibitory molecules may also activate PKCζ and the Par complex.

NG2 treatment increased the binding of Par6 to PKCζ, and this binding too was required for growth inhibition. Since wild-type and CA-Cdc42 but not DN-Cdc42 bind strongly to Par6, the enhanced binding of Par6 to PKCζ caused by NG2 treatment may increase the sensitivity of the kinase to activation by Cdc42. Indeed, overexpression of Par6 in COS cells is sufficient to increase PKCζ activity (Qiu et al., 2000). The physiological modulation of Par6–PKCζ binding shown here may be a novel mechanism for the regulation of the Par complex function by extracellular molecules.

We also showed that NG2 treatment activates Rac1 in CGNs and that this activation is also necessary and sufficient to inhibit neurite extension. Both the activation of Rac1 and the inhibition of growth

require active PKCζ and a phosphorylatable serine residue at position 824 in Par3. Par3 binds TIAM (T-lymphoma invasion and metastasis-inducing protein) and STEF (Sif- and Tiam1-like exchange factor), guanine exchange factors that directly activate Rac1, and this binding can either positively or negatively regulate Rac1 activity. For example, in epithelial cells, Par3 may sequester TIAM away from Rac1, thereby reducing activity (Chen and Macara, 2005). In polarizing hippocampal neurons, however, STEF is bound to the Par complex via Par3 and activates Rac1 in a Cdc42-dependent manner (Nishimura et al., 2005). During polarization and axon specification, Par3 along with PKCζ, STEF, and Rap1B becomes localized at the tip of the neurite that will develop into the axon. Disrupting this distribution causes defects in polarization (Schwamborn and Puschel, 2004; Nishimura et al., 2005; Schwamborn et al., 2007). One consequence of NG2 treatment of CGNs is the accumulation of Par3 in neuronal cell bodies, possibly due to interference with Par3–kif3A interactions (Nishimura et al., 2004). We speculate that the accumulation of Par3 in cell bodies leads to a spatially inappropriate activation of Rac1 and compromised axon extension. Balanced Rac1 and RhoA activity is required for neurite extension (Woo and Gomez, 2006), and disturbances of this balance may explain why CA-Rac1 inhibits neurite growth from CGNs as reported here and rat cortical neurons (Kubo et al., 2002) but promotes growth from embryonic hippocampal neurons (Schwamborn et al., 2007) and postnatal neuronal progenitor cells (Khodosevich and Monyer, 2010). Unbalanced and spatially inappropriate activation of Rac1 activity in damaged axons after SCI may be one reason why transected axons fail to reform growth cones and initiate regrowth (Bradke et al., 2012).

Not all the effects of NG2 on axon growth, however, may be due to inappropriate Rac1 activation. Whereas the expression of CA-Rac1 leads to short neurites with lamellipodial-like extensions, the axons of cells grown on NG2 while short have collapsed growth cones but no lamellipodia (Dou and Levine, 1994; Ughrin et al., 2003). CSPGs and myelin-associated axon growth inhibitors are thought to activate Rho, although recently the significance of this activation for growth inhibition by myelin has been questioned (Park et al., 2010). Although NG2 treatment increases Rho-GTP in CGNs (W. Zhang and J. Levine, unpublished observation), treatment of cells with the ROCK inhibitor Y27632 did not prevent the NG2-induced reduction in Par3–PKCζ binding. PKCζ phosphorylates rodent Par3 at S827 (Lin et al., 2000; Nagai-Tamai et al., 2002), and ROCK phosphorylates Par3 at T833 (Nakayama et al., 2008). Since the expression of a phosphomutant Par3 (S824A) restored normal neurite lengths on NG2 surfaces and prevented the activation of Rac1, we conclude that Rho-activation is not necessary for the NG2-induced, Par3-dependent activation of Rac1. Rather, the activation of Rac1 is dependent upon the activation of PKCζ. It is possible, however, that growth inhibitory molecules such as NG2 activate Rho downstream of PKCζ, and Rho together with Rac1 compromise the function of actin and microtubule-based cytoskeletal motors.

NG2 is one of several CSPGs whose expression is rapidly increased at sites of spinal cord injury (Tang et al., 2003). NG2 has a unique protein structure (Staub et al., 2002) and, unlike other injury-associated CSPGs such as neurocan, aggrecan, and versican, contains relatively low amounts of covalently bound chondroitin sulfate glycosaminoglycan chains. Thus, it is not surprising that NG2 activates intracellular signaling pathways differently than those CSPGs such as neurocan that bind to PTPσ via their GAG chains (Shen et al., 2009). In addition to CSPGs, numerous repulsive axon guidance molecules and myelin-associated inhibitors accumulate at sites of CNS injury (Yiu and He, 2006). While it seems unlikely that there is one common pathway by which these diverse molecules inhibit axon regeneration, several lines of evidence, in addition to the data presented here, point to the Par complex as a potential new and novel intracellular mediator of growth inhibition and repulsive axon guidance. Wnt5a is increased at sites of spinal cord injury and prevents the regeneration of descending corticospinal tract axons in rodents (Liu et al., 2008; Miyashita et al., 2009). Similar to NG2, Wnt5a activates PKCζ (Wolf et al., 2008), promotes the polarization of hippocampal neurons (Zhang et al., 2007), and inhibits the growth of CGNs *in vitro* (Miyashita et al., 2009). Genetic knock-out studies suggest that the phosphatase and tensin homolog (PTEN) plays a major role in preventing nerve regeneration after optic nerve crush (Park et al., 2008) and spinal cord injury (Liu et al., 2010). The exact mechanisms of PTEN-mediated inhibition of regeneration are unknown, but high PTEN activity perturbs Par complex function. In developing hippocampal neurons, overexpression of PTEN reduces PIP3 levels, resulting in a failure to properly target Par3 to axon tips and reduced neuronal polarization (Shi et al., 2003; Ménager et al., 2004). In this regard, it is interesting that knocking down PTEN partially rescues neurons from MAG-induced growth inhibition (Perdigoto et al., 2011).

In summary, we have identified a new role for Par complex proteins in the negative regulation of axonal growth and showed that a major CSPG that accumulates at sites of brain and spinal cord injury (Levine, 1994; Jones et al., 2002) activates PKCζ and the Par complex. Inhibition of axon growth by myelin also depends partially on the activity of PKCζ. These findings emphasize the functional diversity of PKCζ and the Par complex proteins in axonal growth regulation. Further genetic and functional studies will be necessary to fully elucidate the functions of the Par complex in axon regeneration and repair.

References

Arimura N, Kaibuchi K (2007) Neuronal polarity: from extracellular signals to intracellular mechanisms. Nat Rev Neurosci 8:194–205. CrossRef Medline

Asher RA, Morgenstern DA, Fidler PS, Adcock KH, Oohira A, Braistead JE, Levine JM, Margolis RU, Rogers JH, Fawcett JW (2000) Neurocan is upregulated in injured brain and in cytokine-treated astrocytes. J Neurosci 20:2427–2438. Medline

Bashaw GJ, Klein R (2010) Signaling from axon guidance receptors. Cold Spring Harb Perspect Biol 2:a001941. CrossRef Medline

Behl C, Widmann M, Trapp T, Holsboer F (1995) 17-beta estradiol protects neurons from oxidative stress-induced cell death *in vitro*. Biochem Biophys Res Commun 216:473–482. CrossRef Medline

Bradke F, Fawcett JW, Spira ME (2012) Assembly of a new growth cone after axotomy: the precursor to axon regeneration. Nat Rev Neurosci 13:183–193. Medline

Busch SA, Horn KP, Cuascut FX, Hawthorne AL, Bai L, Miller RH, Silver J (2010) Adult NG2+ cells are permissive to neurite outgrowth and stabilize sensory axons during macrophage-induced axonal dieback after spinal cord injury. J Neurosci 30:255–265. CrossRef Medline

Chen X, Macara IG (2005) Par-3 controls tight junction assembly through the Rac exchange factor Tiam1. Nat Cell Biol 7:262–269. CrossRef Medline

Chen YM, Wang QJ, Hu HS, Yu PC, Zhu J, Drewes G, Piwnica-Worms H, Luo ZG (2006) Microtubule affinity-regulating kinase 2 functions downstream of the PAR-3/PAR-6/atypical PKC complex in regulating hippocampal neuronal polarity. Proc Natl Acad Sci U S A 103:8534–8539. CrossRef Medline

Chen ZJ, Ughrin Y, Levine JM (2002) Inhibition of axon growth by oligodendrocyte precursor cells. Mol Cell Neurosci 20:125–139. CrossRef Medline

Chou MM, Hou W, Johnson J, Graham LK, Lee MH, Chen CS, Newton AC, Schaffhausen BS, Toker A (1998) Regulation of protein kinase C [zeta] by PI 3-kinase and PDK-1. Curr Biol 8:1069–1077. CrossRef Medline

Dewald LE, Rodriguez JP, Levine JM (2011) The RE1 binding protein REST

regulates oligodendrocyte differentiation. J Neurosci 31:3470–3483. CrossRef Medline

Dotti CG, Sullivan CA, Banker GA (1988) The establishment of polarity by hippocampal neurons in culture. J Neurosci 8:1454–1468. Medline

Dou CL, Levine JM (1994) Inhibition of neurite growth by the NG2 chondroitin sulfate proteoglycan. J Neurosci 14:7616–7628. Medline

Dou CL, Levine JM (1997) Identification of a neuronal cell surface receptor for a growth inhibitory chondroitin sulfate proteoglycan (NG2). J Neurochem 68:1021–1030. Medline

Etienne-Manneville S, Hall A (2001) Integrin-mediated activation of Cdc42 controls cell polarity in migrating astrocytes through PKC[zeta]. Cell 106:489–498. CrossRef Medline

Fidler PS, Schuette K, Asher RA, Dobbertin A, Thornton SR, Calle-Patino Y, Muir E, Levine JM, Geller HM, Rogers JH, Faissner A, Fawcett JW (1999) Comparing astrocytic cell lines that are inhibitory or permissive for axon growth: the major axon-inhibitory proteoglycan is NG2. J Neurosci 19: 8778–8788. Medline

Gao L, Joberty G, Macara IG (2002) Assembly of epithelial tight junctions is negatively regulated by Par6. Curr Biol 12:221–225. CrossRef Medline

Hasegawa Y, Fujitani M, Hata K, Tohyama M, Yamagishi S, Yamashita T (2004) Promotion of axon regeneration by myelin-associated glycoprotein and Nogo through divergent signals downstream of Gi/G. J Neurosci 24:6826–6832. CrossRef Medline

Hurd TW, Margolis B (2005) Pars and polarity: taking control of Rac. Nat Cell Biol 7:205–207. CrossRef Medline

Jin Z, Strittmatter SM (1997) Rac1 mediates collapsin-1-induced growth cone collapse. J Neurosci 17:6256–6263. Medline

Joberty G, Petersen C, Gao L, Macara IG (2000) The cell-polarity protein Par6 links Par3 and atypical protein kinase C to Cdc42. Nat Cell Biol 2:531–539. CrossRef Medline

Jones LL, Yamaguchi Y, Stallcup WB, Tuszynski MH (2002) NG2 is a major chondroitin sulfate proteoglycan produced after spinal cord injury and is expressed by macrophages and oligodendrocyte progenitors. J Neurosci 22:2792–2803. Medline

Kazanietz MG, Areces LB, Bahador A, Mischak H, Goodnight J, Mushinski JF, Blumberg PM (1993) Characterization of ligand and substrate specificity for the calcium-dependent and calcium-independent protein kinase C isozymes. Mol Pharmacol 44:298–307. Medline

Kazi JU, Soh JW (2007) Isoform-specific translocation of PKC isoforms in NIH3T3 cells by TPA. Biochem Biophys Res Commun 364:231–237. CrossRef Medline

Khodosevich K, Monyer H (2010) Signaling involved in neurite outgrowth of postnatally born subventricular zone neurons *in vitro*. BMC Neurosci 11:18. CrossRef Medline

Kim S, Gailite I, Moussian B, Luschnig S, Goette M, Fricke K, Honemann-Capito M, Grubmüller H, Wodarz A (2009) Kinase-activity-independent functions of atypical protein kinase C in *Drosophila*. J Cell Sci 122:3759–3771. CrossRef Medline

Kubo T, Yamashite T, Yamaguchi A, Sumimoto H, Hosokawa K, Tohyama M (2002) A novel FERM domain including guanine nucleotide exchange factor is involved in rac signaling and regulates neurite remodeling. J Neurosci 22:8504–8513. Medline

Kuhn TB, Brown MD, Wilcox CL, Raper JA, Bamburg JR (1999) Myelin and collapsin-1 induce motor neuron growth cone collapse through different pathways: inhibition of collapse by opposing mutants of Rac1. J Neurosci 19:1965–1975. Medline

Levine JM (1994) Increased expression of the NG2 chondroitin-sulfate proteoglycan after brain injury. J Neurosci 14:4716–4730. Medline

Lin D, Edwards AS, Fawcett JP, Mbamalu G, Scott JD, Pawson T (2000) A mammalian PAR-3-PAR-6 complex implicated in Cdc42/Rac1 and aPKC signalling and cell polarity. Nat Cell Biol 2:540–547. CrossRef Medline

Liu K, Lu Y, Lee JK, Samara R, Willenberg R, Sears-Kraxberger I, Tedeschi A, Park KK, Jin D, Cai B, Xu B, Connolly L, Steward O, Zheng B, He Z (2010) PTEN deletion enhances the regenerative ability of adult corticospinal neurons. Nat Neurosci 13:1075–1081. CrossRef Medline

Liu Y, Wang X, Lu CC, Kerman R, Steward O, Xu XM, Zou Y (2008) Repulsive Wnt signaling inhibits axon regeneration after CNS injury. J Neurosci 28:8376–8382. CrossRef Medline

Macara IG (2004) Parsing the polarity code. Nat Rev Mol Cell Biol 5:220–231. CrossRef Medline

Ménager C, Arimura N, Fukata Y, Kaibuchi K (2004) PIP3 is involved in neuronal polarization and axon formation. J Neurochem 89:109–118. CrossRef Medline

Miyashita T, Koda M, Kitajo K, Yamazaki M, Takahashi K, Kikuchi A, Yamashita T (2009) Wnt-Ryk signaling mediates axon growth inhibition and limits functional recovery after spinal cord injury. J Neurotrauma 26:955–964. CrossRef Medline

Mosthaf L, Kellerer M, Mühlhöfer A, Mushack J, Seffer E, Häring HU (1996) Insulin leads to a parallel translocation of PI-3-kinase and protein kinase C zeta. Exp Clin Endocrinol Diabetes 104:19–24. CrossRef Medline

Nagai-Tamai Y, Mizuno K, Hirose T, Suzuki A, Ohno S (2002) Regulated protein-protein interaction between aPKC and PAR-3 plays an essential role in the polarization of epithelial cells. Genes Cells 7:1161–1171. CrossRef Medline

Nakayama M, Goto TM, Sugimoto M, Nishimura T, Shinagawa T, Ohno S, Amano M, Kaibuchi K (2008) Rho-kinase phosphorylates PAR-3 and disrupts PAR complex formation. Dev Cell 14:205–215. CrossRef Medline

Nishikawa K, Toker A, Johannes FJ, Songyang Z, Cantley LC (1997) Determination of the specific substrate sequence motifs of protein kinase C isozymes. J Biol Chem 272:952–960. CrossRef Medline

Nishimura T, Kato K, Yamaguchi T, Fukata Y, Ohno S, Kaibuchi K (2004) Role of the PAR-3-KIF3 complex in the establishment of neuronal polarity. Nat Cell Biol 6:328–334. CrossRef Medline

Nishimura T, Yamaguchi T, Kato K, Yoshizawa M, Nabeshima Y, Ohno S, Hoshino M, Kaibuchi K (2005) PAR-6-PAR-3 mediates Cdc42-induced Rac activation through the Rac GEFs STEF/Tiam1. Nat Cell Biol 7:270–277. CrossRef Medline

Norton WT, Poduslo SE (1973) Myelination in rat brain: method of myelin Isolation. J Neurochem 21:749–757. CrossRef Medline

Ozdamar B, Bose R, Barrios-Rodiles M, Wang HR, Zhang Y, Wrana JL (2005) Regulation of the polarity protein Par6 by TGFbeta receptors controls epithelial cell plasticity. Science 307:1603–1609. CrossRef Medline

Park KJ, Grosso CA, Aubert I, Kaplan DR, Miller FD (2010) p75NTR-dependent, myelin-mediated axonal degeneration regulates neural connectivity in the adult brain. Nat Neurosci 13:559–566. CrossRef Medline

Park KK, Liu K, Hu Y, Smith PD, Wang C, Cai B, Xu B, Connolly L, Kramvis I, Sahin M, He Z (2008) Promoting axon regeneration in the adult CNS by modulation of the PTEN/mTOR pathway. Science 322:963–966. CrossRef Medline

Perdigoto AL, Chaudhry N, Barnes GN, Filbin MT, Carter BD (2011) A novel role for PTEN in the inhibition of neurite outgrowth by myelin-associated glycoprotein in cortical neurons. Mol Cell Neurosci 46: 235–244. CrossRef Medline

Powell EM, Fawcett JW, Geller HM (1997) Proteoglycans provide neurite guidance at an astrocyte boundary. Mol Cell Neurosci 10:27–42. CrossRef Medline

Qiu RG, Abo A, Steven Martin G (2000) A human homolog of the *C. elegans* polarity determinant Par-6 links Rac and Cdc42 to PKCzeta signaling and cell transformation. Curr Biol 10:697–707. CrossRef Medline

Ramón y Cajal S (1928) Degeneration and regeneration of the nervous system. London: Oxford UP.

Romanelli A, Martin KA, Toker A, Blenis J (1999) p70 S6 kinase is regulated by protein kinase C zeta and participates in a phosphoinositide 3-kinase regulated signalling complex. Mol Cell Biol 19:2921–2928. Medline

Schwab JM, Bernard F, Moreau-Fauvarque C, Chédotal A (2005) Injury reactive myelin/oligodendrocyte-derived axon growth inhibition in the adult mammalian central nervous system. Brain Res Rev 49:295–299. CrossRef Medline

Schwamborn JC, Püschel AW (2004) The sequential activity of the GTPases Rap1B and Cdc42 determines neuronal polarity. Nat Neurosci 7:923–929. CrossRef Medline

Schwamborn JC, Müller M, Annemarie HM Becker, Püschel AW (2007) Ubiquitination of the GTPase Rap1B by the ubiquitin ligase Smurf2 is required for the establishment of neuronal polarity. EMBO J 26:1410–1422. CrossRef Medline

Shen Y, Tenney AP, Busch SA, Horn KP, Cuascut FX, Liu K, He Z, Silver J, Flanagan JG (2009) PTPsigma is a receptor for chondroitin sulfate proteoglycan, an inhibitor of neural regeneration. Science 326:592–596. CrossRef Medline

Shi SH, Jan LY, Jan YN (2003) Hippocampal neuronal polarity specified by

spatially localized mPar3/mPar6 and PI 3-kinase activity. Cell 112:63–75. CrossRef Medline

Sivasankaran R, Pei J, Wang KC, Zhang YP, Shields CB, Xu XM, He Z (2004) PKC mediates inhibitory effects of myelin and chondroitin sulfate proteoglycans on axonal regeneration. Nat Neurosci 7:261–268. CrossRef Medline

Snow DM, Lemmon V, Carrino DA, Caplan AI, Silver J (1990) Sulfated proteoglycans in astroglial barriers inhibit neurite outgrowth *in vitro*. Exp Neurol 109:111–130. CrossRef Medline

Standaert ML, Bandyopadhyay G, Perez L, Price D, Galloway L, Poklepovic A, Sajan MP, Cenni V, Sirri A, Moscat J, Toker A, Farese RV (1999) Insulin activates protein kinases C-zeta and C-lambda by an autophosphorylation-dependent mechanism and stimulates their translocation to GLUT4 vesicles and other membrane fractions in rat adipocytes. J Biol Chem 274: 25308–25316. CrossRef Medline

Standaert ML, Bandyopadhyay G, Kanoh Y, Sajan MP, Farese RV (2001) Insulin and PIP3 activate PKC-zeta by mechanisms that are both dependent and independent of phosphorylation of activation loop (T410) and autophosphorylation (T560) sites. Biochemistry 40:249–255. CrossRef Medline

Staub E, Hinzmann B, Rosenthal A (2002) A novel repeat in the melanoma-associated chondroitin sulfate proteoglycan defines a new protein family. FEBS Lett 527:114–118. CrossRef Medline

Tan AM, Colletti M, Rorai AT, Skene JH, Levine JM (2006) Antibodies against the NG2 proteoglycan promote the regeneration of sensory axons within the dorsal columns of the spinal cord. J Neurosci 26:4729–4739. CrossRef Medline

Tang X, Davies JE, Davies SJ (2003) Changes in distribution, cell associations, and protein expression levels of NG2, neurocan, phosphacan, brevican, versican V2, and tenascin-C during acute to chronic maturation of spinal cord scar tissue. J Neurosci Res 71:427–444. CrossRef Medline

Tessier-Lavigne M, Goodman CS (1996) The molecular biology of axon guidance. Science 274:1123–1133. CrossRef Medline

Tillet E, Ruggiero F, Nishiyama A, Stallcup WB (1997) The membrane-spanning proteoglycan NG2 binds to collagens V and VI through the central nonglobular domain of its core protein. J Biol Chem 272: 10769–10776. CrossRef Medline

Ughrin YM, Chen ZJ, Levine JM (2003) Multiple regions of the NG2 proteoglycan inhibit neurite growth and induce growth cone collapse. J Neurosci 23:175–186. Medline

Vielmetter J, Stolze B, Bonhoeffer F, Stuermer CA (1990) *In vitro* assay to test differential substrate affinities of growing axons and migratory cells. Exp Brain Res 81:283–287. Medline

Wang HR, Zhang Y, Ozdamar B, Ogunjimi AA, Alexandrova E, Thomsen GH, Wrana JL (2003) Regulation of cell polarity and protrusion formation by targeting RhoA for degradation. Science 302:1775–1779. CrossRef Medline

Wolf AM, Lyuksyutova AI, Fenstermaker AG, Shafer B, Lo CG, Zou Y (2008) Phosphatidylinositol-3-kinase-atypical protein kinase C signaling is required for Wnt attraction and anterior-posterior axon guidance. J Neurosci 28:3456–3467. CrossRef Medline

Woo S, Gomez TM (2006) Rac1 and rhoA promote neurite outgrowth through formation and stabilization of growth cone contact points. J Neurosci 26:1418–1428. CrossRef Medline

Yamanaka T, Horikoshi Y, Suzuki A, Sugiyama Y, Kitamura K, Maniwa R, Nagai Y, Yamashita A, Hirose T, Ishikawa H, Ohno S (2001) PAR-6 regulates aPKC activity in a novel way and mediates cell-cell contact-induced formation of the epithelial junctional complex. Genes Cells 6:721–731. CrossRef Medline

Yang H, Lu P, McKay HM, Bernot T, Keirstead H, Steward O, Gage FH, Edgerton VR, Tuszynski MH (2006a) Endogenous neurogenesis replaces oligodendrocytes and astrocytes after primate spinal cord injury. J Neurosci 26:2157–2166. CrossRef Medline

Yang Z, Suzuki R, Daniels SB, Brunquell CB, Sala CJ, Nishiyama A (2006b) NG2 glial cells provide a favorable substrate for growing axons. J Neurosci 26:3829–3839. CrossRef Medline

Yi JJ, Barnes AP, Hand R, Polleux F, Ehlers MD (2010) TGF-beta signaling specifies axons during brain development. Cell 142:144–157. CrossRef Medline

Yiu G, He Z (2006) Glial inhibition of CNS axon regeneration. Nat Rev Neurosci 7:617–627. CrossRef Medline

Zhang H, Macara IG (2008) The PAR-6 polarity protein regulates dendritic spine morphogenesis through p190 RhoGAP and the Rho GTPase. Dev Cell 14:216–226. CrossRef Medline

Zhang X, Zhu J, Yang GY, Wang QJ, Qian L, Chen YM, Chen F, Tao Y, Hu HS, Wang T, Luo ZG (2007) Dishevelled promotes axon differentiation by regulating atypical protein kinase C. Nat Cell Biol 9:743–754. CrossRef Medline